AD-A110 397 ARMY ELECTRONICS RESEARCH AND DEVELOPMENT COMMAND WS--ETC F/G 7/4
WATER VAPOR ABSORPTION COEFFICIENTS AT HF LASER WAVELENGTHS. PA--ETC(U)
NOV 81 R L SPELLICY, L J CROW, K O WHITE

UNCLASSIFIED ERADCOM/ASL-TR-0099 NL

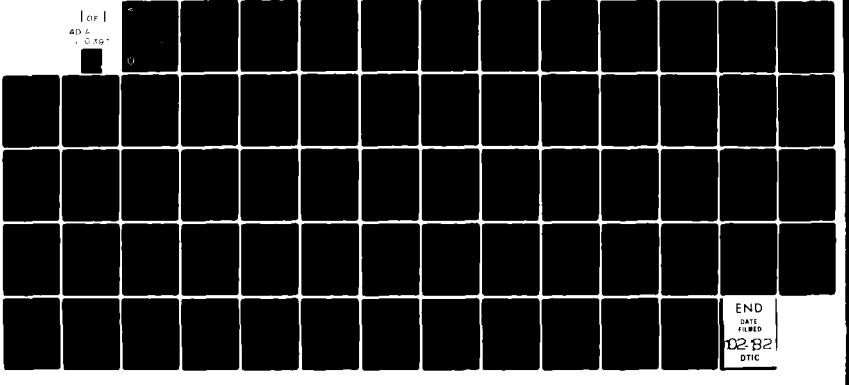

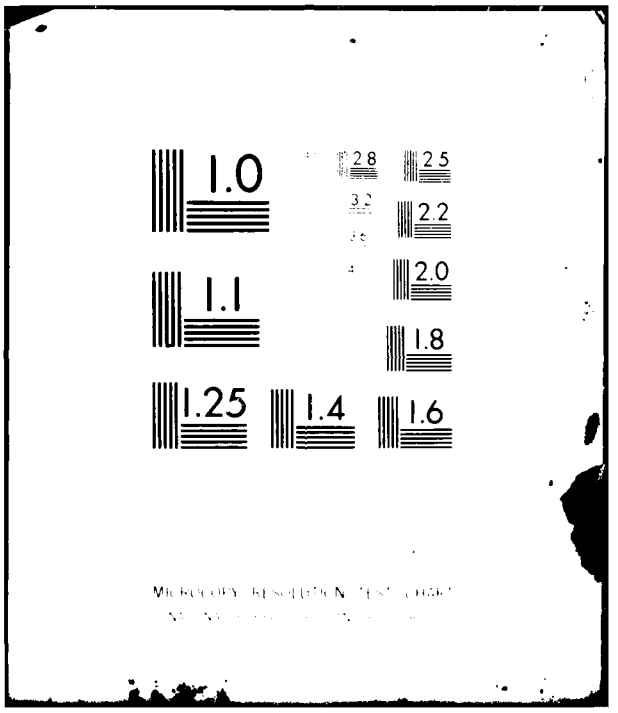
1.0
2.8
2.5
3.2
2.2
2.0
1.1
1.8
1.25
1.4
1.6

-TR-0099

WATER VAPOR ABSORPTION COEFFICIENTS AT HF LASER WAVELENGTHS

PART II: DEVELOPMENT OF THE MEASUREMENT SYSTEM AND MEASUREMENTS AT SIMULATED ALTITUDES TO 10 KM

NOVEMBER 1981

By

Robert L. Spellicy
OptiMetrics, Inc.
Ann Arbor, MI

Laura J. Crow
Kenneth O. White

US Army Electronics Research and Development Command
Atmospheric Sciences Laboratory
White Sands Missile Range, NM 88002

NOTICES

Disclaimers

The findings in this report are not to be construed as an official Department of the Army position, unless so designated by other authorized documents.

The citation of trade names and names of manufacturers in this report is not to be construed as official Government indorsement or approval of commercial products or services referenced herein.

Disposition

Destroy this report when it is no longer needed. Do not return it to the originator.

SECURITY CLASSIFICATION OF THIS PAGE *(When Data Entered)*

REPORT DOCUMENTATION PAGE

READ INSTRUCTIONS BEFORE COMPLETING FORM

1. REPORT NUMBER: ASL-TR-0099	2. GOVT ACCESSION NO.: AD-A110 347
3. RECIPIENT'S CATALOG NUMBER	
4. TITLE *(and Subtitle)*: WATER VAPOR ABSORPTION COEFFICIENTS AT HF LASER WAVELENGTHS PART II: DEVELOPMENT OF THE MEASUREMENT SYSTEM AND MEASUREMENTS AT SIMULATED ALTITUDES TO 10 KM	5. TYPE OF REPORT & PERIOD COVERED: Final Report
	6. PERFORMING ORG. REPORT NUMBER
7. AUTHOR(s): Robert L. Spellicy, OptiMetrics, Inc. Laura J. Crow & Kenneth O. White, ASL	8. CONTRACT OR GRANT NUMBER(s)
9. PERFORMING ORGANIZATION NAME AND ADDRESS: US Army Atmospheric Sciences Laboratory White Sands Missile Range, NM 88002	10. PROGRAM ELEMENT, PROJECT, TASK AREA & WORK UNIT NUMBERS: DA Task No. 1L161102B53A
11. CONTROLLING OFFICE NAME AND ADDRESS: US Army Electronics Research and Development Command Adelphi, MD 20783	12. REPORT DATE: November 1981 13. NUMBER OF PAGES: 64
14. MONITORING AGENCY NAME & ADDRESS*(if different from Controlling Office)*	15. SECURITY CLASS. *(of this report)*: UNCLASSIFIED 15a. DECLASSIFICATION/DOWNGRADING SCHEDULE

16. DISTRIBUTION STATEMENT *(of this Report)*

Approved for public release; distribution unlimited.

17. DISTRIBUTION STATEMENT *(of the abstract entered in Block 20, if different from Report)*

18. SUPPLEMENTARY NOTES

19. KEY WORDS *(Continue on reverse side if necessary and identify by block number)*

Absorption
Water vapor
Laser
Infrared
HF laser
Atmospheric optics

20. ABSTRACT *(Continue on reverse side if necessary and identify by block number)*

A unique differential photoacoustic system is described along with water vapor absorption measurements made at HF laser lines. The photoacoustic system is capable of determining absorption coefficients to 5×10^{-3} km^{-1}. Comparisons of the data with calculated values based on a modified Lorentz profile with an augmented line wing and the latest atmospheric absorption line compilation showed good agreement for all laser lines at high pressures (N700 torr) with some discrepancies at lower pressures.

DD FORM 1 JAN 73 1473 EDITION OF 1 NOV 65 IS OBSOLETE

SECURITY CLASSIFICATION OF THIS PAGE *(When Data Entered)*

BLANK PAGE

CONTENTS

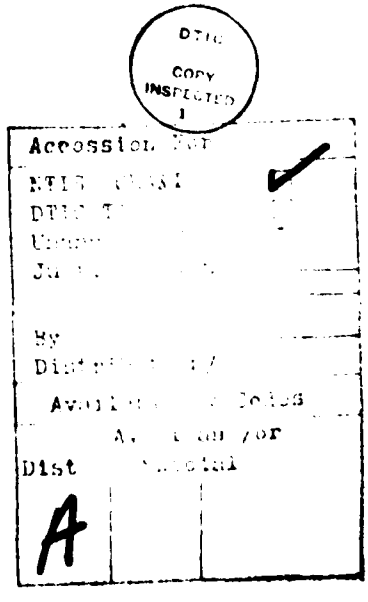

RE: Classified References, Distribution Unlimited.
No *Change* in distribution statement per Mr. Buck Sims, AASL/DELAS-DM-A

LIST OF TABLES

LIST OF FIGURES

List of Figures (cont)

INTRODUCTION

The HF laser is attractive for a variety of military applications because of its relatively short wavelength and its potential for high output powers. Unfortunately, its transition frequencies fall in or near the 2.7μm water vapor bands, resulting in severe atmospheric attenuation for all but extremely dry, low altitude environments. At upper altitudes, however, where the water content of the atmosphere is low, this laser should exhibit good propagation characteristics.

Although it is possible to use line-by-line (HITRAN type) procedures to evaluate absorption coefficients at HF laser line positions, the accuracy of these calculated coefficients is uncertain.[1] This is the case since in evaluating coefficients at discrete laser wavelengths, the calculated values are highly sensitive to the strengths, positions, and widths of spectral lines in the immediate vicinity of the laser frequency. As a result, small errors in these parameters can significantly alter the calculated coefficients as well as their pressure/temperature dependence. In addition, to accurately evaluate coefficients in as dense a spectral region as the 2.7μm water bands, an accurate knowledge of the overall line shape is critical if one is to properly account for the wing contributions of the multitude of lines around the laser frequency.

To determine the accuracy of these calculational procedures, a previous experimental program was undertaken which measured absorption coefficients at a number of HF laser lines as a function of water content, temperature, and total pressure.[1] Comparisons of these measured values with line-by-line calculations indicated that agreement could be obtained only if modifications were made to the calculational data base (the Air Force Geophysics Laboratory [AFGL] atmospheric absorption line compilation)[2] and if a modified line profile were used.

Since the measurements performed under the previous program were limited to conditions corresponding to altitudes of 7 km or less, the current program was undertaken to extend these measurements and to determine the validity of the modified calculational procedures at yet higher altitudes. This report presents details of a photoacoustic system developed to perform these measurements, along with data collected with this system on HF laser lines $P_1(7)$, $P_2(5)$, $P_2(6)$, $P_2(7)$, and $P_2(8)$ for mole fractions and pressures corresponding to altitudes up to 10 km.

---

[1]Wendell R. Watkins et al, 1978, Water Vapor Absorption Coefficients At HF Laser Wavelengths, Part I: Atmospheric Conditions Corresponding to Altitudes up to 7 km, ASL-TR-0007, US Army Atmospheric Sciences Laboratory, White Sands Missile Range, NM.

[2]R. A. McClatchey et al, 1973, AFCRL Atmospheric Absorption Line Parameter Compilation, AFGL-TR-73-0096, Air Force Geophysics Laboratory, Hanscom AFB, MA.

Appendix A contains background into the theory of measuring absorption coefficients by photoacoustic detection with a spectrophone. A discussion of the system and the procedures developed for its calibration and use are presented in subsequent sections of this report.

EXPERIMENTAL SYSTEM

The Optical System

The optical system constructed for spectrophone absorption measurements is shown schematically in figure 1, in which a pulsed Lumonics laser was used as a source of IR radiation. Because of the strong RF fields associated with the discharge of this laser, it was placed about 30 m away from the actual spectrophone system and its output beam controlled with a servo-operated flat mirror (F3). Since the near field output pattern of this laser was a donut shaped mode, mirror F3 could be pierced without any loss of energy and an HeNe beam coincident with the IR beam allowed for visual alignment of the optics. Once propagated to the optics table containing the remainder of the system, the beam was reduced in size and recollimated using two spherical mirrors S1 and S2. Flat mirrors (F5, F6) were then used, in conjunction with a pair of irises placed on either side of the spectrophone cavity, to align the beam with the axis of the spectrophone. Mirror F7 reflected the beam back on itself, double passing the cavity, and a portion of the reemerging beam was split off to monitor the laser power.

Because of the distance that the IR beam traveled in getting to the optics table, turbulence in the laboratory air caused the beam to jitter. This had little if any effect on the spectrophone itself since the beam size was small compared to the 1.59-cm bore in the cavity. In monitoring the laser energy, however, small beam motions significantly altered the output of the pyroelectric detector. To eliminate these variations, an off-axis parabola (P1) was used to image the fraction of the beam reflected off the beam splitter (BS) onto a diffusion plate (D) placed 2.5 to 5 cm in front of the pyroelectric detector. Since the diffuser had a fairly broad forward-scattering lobe, small motions of the beam on this plate had virtually no effect on the detector signal.

The Spectrophone

As shown in figure 2, the spectrophone assembly consisted of an outer vacuum jacket which contained the resonant subchamber or photoacoustic detector. The outer jacket was designed by Charles Bruce.[3] It incorporates a damping

---

[3]C. W. Bruce, 1976, Development of Spectrophones for CW and Pulsed Radiation Sources, ECOM-5802, Atmospheric Sciences Laboratory, US Army Electronics Command, White Sands Missile Range, NM.

chamber behind the windows and damping discs to decouple false window signals from the resonant subchamber.

The resonant subchamber used in this study evolved after several iterations of prototype design and testing. All of the designs considered, however, were cylindrical chambers with small inside-diameter-to-length ratios, so that they could be operated at their fundamental longitudinal resonance at frequencies in the kilohertz range. After several different designs were tested, a unique differential subchamber was built with electret microphones at the ends and in the center (figure 3). When operated in a differential mode, the signals from the end microphones were averaged and subtracted from those of the central microphones. Since the fundamental longitudinal mode of this chamber had a maximum pressure variation at the center and pressure nodes at or near the ends, this subtraction effectively canceled signals common to all microphones while leaving the signal arising from the fundamental mode relatively unattenuated. This had the advantage of substantially reducing unwanted system noise arising from window absorption effects and/or RF interference from the laser trigger.

Tests of this system indicated that RF pickup signals were not at all in evidence when the system was operated differentially, while without end-microphone subtraction laser trigger noise generated a 0.45-mV spike on the leading edge of the output waveform which itself had an amplitude of only 0.05 mV. Background acoustic noise was also highly attenuated as was seen by deliberately injecting noise into the system using either a speaker or the pump used to circulate gases through the spectrophone chamber. Without end-microphone subtraction, the resonant signal was almost completely concealed by this extraneous noise, while with subtraction this signal--although noisy--was clearly discernible.

Tests were run on this differential system to determine detection thresholds, using water vapor fills for which measured absorption coefficients were available,[1] to determine calibration factors and pure nitrogen fills to establish background noise levels. The results of these tests are shown in figure 4, in which the noise equivalent absorption coefficient is plotted against nitrogen pressure for the various laser lines. Surprisingly, this data indicated that the background level increased with increasing pressure and was a function of the laser line used. Although the exact origin of these signals is not known, it is believed that they arose from absorption in the chamber windows, since their magnitudes varied as the inverse of the H_2O/CO_2 absorption for the various lines. Thus, the lines experiencing less H_2O/CO_2 attenuation would be substantially stronger and less diffuse after traversing

---

[1]Wendell R. Watkins et al, 1978, Water Vapor Absorption Coefficients At HF Laser Wavelengths, Part I: Atmospheric Conditions Corresponding to Altitudes up to 7 km, ASL-TR-0007, US Army Atmospheric Sciences Laboratory, White Sands Missile Range, NM.

the 30-m path from the laser to the spectrophone system than lines with larger H_2O/CO_2 attenuations. Attempts to further reduce these background levels proved unsuccessful.

The Gas Fill/Monitoring System

Since relatively low dew-point fills were to be used in the spectrophone to simulate high altitude conditions, a special gas filling and monitoring system had to be constructed to maintain stable, well-known fill conditions. The reservoir system of figure 5 was developed as a source of moderate-to-low dew-point nitrogen/oxygen which could be added to the spectrophone as required to maintain a given low dew-point fill. To charge the reservoir with moderate dew-point gas, it was initially filled with pure nitrogen (and/or oxygen) to a pressure higher than that required for a series of spectrophone fills. This gas was then circulated through a water bath with throttling and by-pass valves (1,2,3), thus adding water vapor to the flow. If desired, a portion of this gas could be extracted and its dew point monitored using the dew-point sensor incorporated into the spectrophone circulation system. Since the volume of the reservoir was approximately 30 times that of the spectrophone, a full reservoir could be used for several series of spectrophone fills.

The spectrophone gas control system is shown in figure 6. A primary vacuum pump (1) was used to evacuate the spectrophone, the gas fill lines, and the capacitance manometers. During evacuation, the system vacuum could be monitored with thermocouple gauges TC1, TC2, and TC3, whose positions were chosen so that the vacuum integrity of the various legs of the system could be routinely monitored. A subsystem consisting of a circulating pump (CP), thermocouple gauge 1 (TC1), and a dew-point meter (DP) was used to flow the spectrophone gas charge across the dew-point sensor to determine its water vapor partial pressure. It also circulated this gas while adding buffer gases to insure homogeneous mixing of the species. The spectrophone fill pressure was monitored using both 0- to 100-torr and 0- to 1000-torr capacitance manometers. A second vacuum system tied onto pump 2 was used to evacuate the region between inner and outer spectrophone windows so that the system could be used at low temperatures without building up frost or condensation on the windows.

For a given fill, the system was initially evacuated using pump 1, after which the circulating pump was started and gas introduced from the reservoir until the approximate dew point of interest was achieved. Buffer gases were then slowly bled into the circulating stream to bring the system up to the desired total pressure. The resulting gas mixture was then circulated, its dew point monitored, and buffer/reservoir gases added as required until a stable fill was achieved. Once the fill appeared to be stable, the spectrophone was valved off and absorption measurements initiated.

The Data Acquisition System

As indicated in equation (A-11) in appendix A, the pressure response of the photoacoustic system divided by the input laser power is directly proportional to the absorption coefficient. Determination of coefficients therefore requires measurement of both the spectrophone "signal" and the laser power. To acquire, digitize, and store these signals, the computer-controlled data system of figure 7 was used. The heart of this system was an HP 2100 computer with several 20-kHz analogue-to-digital (A-to-D) input channels. The A-to-D card in the computer was set up to operate in a paced mode so that while the CPU was requesting data from a given channel, a single data point was digitized and transferred each time an appropriate external trigger pulse was received. With this configuration, the computer software controlled the accessing of the various channels as well as the number of data points taken from each, while the external pacer pulses actually initiated data collection and controlled the data-taking rate.

Since a pulsed laser was used with this system, data collection had to be synchronized with the arrival of each laser pulse. To do this, the pyroelectric detector (used to monitor the laser power) was also used to trigger a set of gate circuits which actually controlled the timing of the system. As shown in figure 8, one of the gate circuits turned on a waveform generator and a pulse generator which supplied pacer pulses to the A-to-D card, initiating data collection on the spectrophone channel--the first channel accessed by the CPU. Also, since the laser power had to be recorded at the same time that the spectrophone signal was being digitized, a second set of gate circuits placed a peak-and-hold circuit in its sample mode for 50μs to acquire the peak of the laser pulse, and then in its hold mode for 70 ms so that the CPU could digitize this value after completion of the spectrophone signal digitization. Both of these signals having been recorded, the gate circuits would shut off the waveform/pulse generators and reset the peak-and-hold circuit in preparation for the next laser pulse, typically occurring 1 s later.

The software implemented on the HP 2100 was set up to optionally collect two different types of data and followed the logic of the flowchart shown in figure 7. Initially, this program interacted with the operator to set up a series of parameters defining the conditions for the specific test as well as parameters relating to the data to be collected from the spectrophone and pyroelectric detector channels. Once this was done, the program would wait for a prompt. Then it would access the spectrophone channel digitizing the desired number of points in the output waveform as soon as the gate circuit supplied the necessary pacer pulses. After digitization of the spectrophone signal, the CPU would immediately switch to the pyroelectric channel and record the laser pulse height as stored in the peak-and-hold circuit. At this point, the software would store the data for the single laser pulse in one of two ways:

1. The actual waveform recorded from the spectrophone would be divided by the pyroelectric peak voltage and summed into a data array, or

2. Pertinent parameters defining the spectrophone "signal" would be evaluated from the waveform and these parameters output to the CRT-terminal in the form of "signal" versus laser power plots.

This process would be repeated for each laser pulse until the desired number of laser pulses had been processed. Then one of two possible options was again followed, depending on whether option 1 or 2 above was chosen for the data collection. If option 1 was used, an average waveform was simply generated and displayed along with values for the waveform peak amplitude, the average laser power, etc., as determined directly from the data. If option 2 was chosen, the software would do a least squares fit to the displayed "signal" versus energy points and display the parameters of this fit.

Once this process was complete, the program could be restarted, either before or after saving the data in a disc file, or the data taking session could be simply terminated.

In effect, option 1 generated an average energy-normalized waveform which could be used for diagnostic purposes or, with further processing, for evaluation of absorption coefficients. Option 2 did not preserve the waveform itself, only those parameters derivable from it (for example, peak amplitude, integrated area, etc.). Option 2 then determined the "signal"-to-power ratio by doing a least squares fit to the data for individual laser pulses. As will be seen below, this latter option was found to be the most reliable for routine data collection.

Calibration and Data Collection Procedures

Using a pulsed laser source in conjunction with an acoustically resonant spectrophone cavity, the output waveform is a damped oscillatory function such as that shown in figure 9. The parameter which must be derived from this waveform is the peak pressure variation normalized to the laser power. To determine this value, several different approaches were evaluated including: measurement of the peak amplitude directly from the observed waveform, measurement of the integrated area of the modulus squared of the waveform, and measurement of the peak and half-width of the resonant frequency spike in the power spectrum of the waveform. The latter two approaches were theoretically preferable because they evaluated the peak amplitude using all data points of the waveform instead of a single point. However, they were less reliable in practice because of the difficulties involved in accurately measuring the pressure-dependent time constants associated with buildup and decay of the pressure wave in the resonant cavity. (These constants were required in order to extract the peak pressure amplitude from either of these measurements.) As a result, the direct approach of measuring the maximum amplitude of the waveform was used. To minimize the effects of noise on these measurements, however, the ratio of peak amplitude to laser power was determined by plotting the amplitude against laser power for a large number of pulses (as shown in figures 10 and 11). This was done while deliberately attenuating the laser beam using neutral density filters to generate a spread in the points. Once collected, a straight line was least-squares fit to the data and the slope,

intercept, and standard deviation of the fit computed. The data was then scanned and points falling greater than two standard deviations away from the curve were flagged (by enclosing them in boxes) and a final fit made ignoring these points. (This iterative process was primarily intended to eliminate extraneous points introduced by frequent false triggering or double triggering by the laser.) The desired signal-to-power ratio was then given by the slope of the resulting curve, while the intercept represented a DC offset in the system which typically varied with spectrophone amplifier gain setting.

As shown in reference 1, absorption coefficients for HF laser lines $P_1(6)$ and $P_2(6)$ may be accurately evaluated using line-by-line procedures in conjunction with a modified line profile and an augmented AFGL absorption line tabulation. Consequently, the spectrophone system used here was calibrated by measuring the signal-to-energy ratio at laser line $P_2(6)$ and correlating this ratio with absorption coefficients calculated for this laser line at the appropriate fill conditions. Figure 12 shows an example of a typical calibration curve obtained in this way for a variety of water vapor fills.

EXPERIMENTAL DATA

Experimental Data on HF Laser Lines

In the present program experimental data were collected on HF laser lines $P_1(7)$, $P_2(5)$, $P_2(6)$, $P_2(7)$, and $P_2(8)$ using water vapor partial pressures of 0.464, 0.182, and 0.054 torr at total pressures of 700, 500, 250, and 125 torr. The results of these measurements are presented in table 1, where the relative values for the lines have been converted to absolute coefficients using the calculated values shown for laser line $P_2(6)$. For laser line $P_2(8)$ only 0.464 torr data were collected because of the high background noise level observed for this line (figure 4). Since for all the measurements the water vapor partial pressure was much smaller than the total pressure, the observed coefficients for a given line should vary linearly with water vapor pressure at constant total pressure. If the modified line profile discussed in reference 1 is assumed correct for the water lines in the HF region, it may be shown that the total absorption coefficient at frequency ν is given by:

$$K(\nu) = P_s \left\{ C \sum_i \frac{S_i \gamma_i P_e}{\pi[(\nu - \nu_i)^2 + \gamma_i^2 P_e^2]} + C' \sum_j \frac{S_j P_e^{n-1} \gamma_j^{n-1}}{(\nu - \nu_j)^n} \right\} \qquad (1)$$

where s_i is the strength of the i^{th} spectral line, γ_i the pressure-broadened half-width of this line, ν the computational frequency, ν_i the line center frequency of the i^{th} line, c and c' normalization constants, n a fit parameter, P_s the absorbing gas specie partial pressure, and P_e the effective broadening pressure. The line profile used in deriving this expression is effectively a composite of two functional forms, one appropriate for near

TABLE 1. OBSERVED ABSORPTION COEFFICIENTS AND LINEAR SQUARES FIT VALUES*

Line $P_1(7)$

Total Pressure (torr)	Water Vapor Pressure (torr)					
	0.054		0.182		0.464	
	Fit	Obs.	Fit	Obs.	Fit	Obs.
125	0.0343	0.0373	0.115	0.117	0.295	0.294
250	0.0552	0.0590	0.186	0.184	0.474	0.475
500	0.0973	0.103	0.328	0.317	0.836	0.840
700	0.133	0.143	0.448	0.453	1.140	1.140

Line $P_2(5)$

Total Pressure (torr)	Water Vapor Pressure (torr)					
	0.054		0.182		0.464	
	Fit	Obs.	Fit	Obs.	Fit	Obs.
125	0.0455	0.0453	0.153	0.153	0.391	0.391
250	0.0794	0.0833	0.267	0.269	0.682	0.681
500	0.1397	0.1460	0.471	0.488	1.200	1.193
700	0.1870	0.196	0.630	0.673	1.607	1.590

*As a function of total pressure water vapor partial pressure. All entries are per kilometer.

Table 1 (cont)

Line $P_2(6)$

Total Pressure (torr)	Water Vapor Pressure (torr)					
	0.054		0.182		0.464	
	Fit	Obs.	Fit	Obs.	Fit	Obs.
125	0.0365	0.0362	0.123	0.122	0.314	0.314
250	0.0667	0.0665	0.225	0.224	0.574	0.574
500	0.122	0.122	0.412	0.412	1.052	1.052
700	0.164	0.164	0.552	0.551	1.407	1.407

Line $P_2(7)$

Total Pressure (torr)	Water Vapor Pressure (torr)					
	0.054		0.182		0.464	
	Fit	Obs.	Fit	Obs.	Fit	Obs.
125	0.005	0.009	0.0167	0.0192	0.0427	0.0413
250	0.0095	0.0106	0.0322	0.0336	0.0820	0.0813
500	0.0165	0.0190	0.0556	0.0567	0.142	0.141
700	0.0224	0.0250	0.0757	0.800	0.193	0.191

Line $P_2(8)$

Total Pressure (torr)	Water Vapor Pressure (torr)	
	0.464	
	Fit	Obs.
125	-	0.010
250	-	0.020
500	-	0.028
700	-	0.032

wings of spectral lines ($\nu - \nu_i \leq 3\gamma_i$) and one appropriate for far wings ($\nu - \nu_i > 3\gamma_i$). As a result, equation 1 contains two summations; in the first the sum over i includes all lines less than three half-widths from the laser frequency (ν), while in the second the sum over j includes all lines outside this range. Since the effective broadening pressure P_e is given by

$$P_e = P_T + (\beta - 1)P_s \tag{2}$$

where P_T is the total pressure and β the self-to-foreign broadening ratio, P_e effectively reduces to P_T whenever P_T is much greater than P_s. This being the case, the sums in equation (1) are constant for a given laser line at constant total pressure, and $K(\nu)$ should vary as

$$K(\nu) = m(P_t, \nu)P_s \tag{3}$$

Using this linear dependence, least squares fits were made to the data as shown in figures 13 and 14. The absorption coefficients obtained from these fits have been included in table 1 along with the observed data. As may be seen from this table, the linear fits did not significantly alter the coefficient values for any of the laser lines except $P_2(7)$. This particular line, however, not only exhibited low water vapor absorption, but also suffered from a high background noise level. The background noise has its greatest effect on the smaller coefficient values, tending to asymptote the data curve to a nonzero value at zero pressure. Fitting to a function such as equation (2) weights the slope value most heavily with the higher pressure data, which is least affected by this noise and hence in the more linear portion of the curve. Values determined from these least squares fits should therefore be more reliable than the raw data at the low absorption levels.

The variation of the slopes of these curves (m) with total pressure (P_t) will generally not be linear, however, since terms involving P_e, P_e^2, and P_e^{n-1} occur in equation (1). If the absorption at a given laser line is dominated by nearby spectral lines, so that the first term of this equation is the significant contributor, then $K(\nu)$ should vary as P_e when $(\nu - \nu_i)^2 > \gamma_i^2 P_e^2$ and slower than P_e when $(\nu - \nu_i)^2 \leq \gamma_i^2 P_e^2$. On the other hand, if $K(\nu)$ is strictly wing dominated, so that the second term is the most significant, the slopes of the curves (m) should vary as P_e^{n-1}. Since in either case m should vary as some power of P_e (or effectively P_t for the present data), least

square fits of the m values as a function of total pressure were made using a function of the form

$$m = C\, P_t^{\alpha} \tag{4}$$

The results of these fits are shown in figures 15 and 16 for the various laser lines. It may be seen from these figures that equation (3) does represent the data well and may therefore be used to interpolate between data points as a function of total pressure. It is also worth noting that the powers of P_t determined for lines $P_2(5)$ and $P_2(7)$ are very close to $(n - 1) = 0.88$. This value was determined in reference 1 to give the best agreement with observations when using equation (1) to compute water vapor/HF-laser absorption coefficients.* Since these laser lines are known to fall in valleys between water vapor absorption lines, it is tempting to state that this agreement supports the modified wing behavior of equation (1). However, it is possible that, by calibrating against calculated coefficients for line $P_2(6)$, the data have been somehow biased with this far-wing pressure dependence. To resolve this question, data should be generated either by using a totally different measurement scheme or by calibrating the spectrophone with a different molecular specie.

Comparisons with Calculations

The primary objective of this program was to determine the validity of line-by-line procedures in computing HF-laser-line absorption coefficients. As a result, line-by-line methods were used to compute absorption coefficients for each of the laser lines at each of the observation conditions. In effect, these calculations used equation (1) in conjunction with line parameters found in the 1980 AFGL atmospheric absorption line compilation.[2] Details of the procedures used are discussed in reference 1 and will not be repeated here. However, it should be noted that:

1. All lines within 20 cm^{-1} of the laser frequency have been included in the computation.

---

*The fact that line $P_1(7)$ exhibits a different behavior may be explained by its almost exact coincidence with two moderate strength water vapor lines.

[2]R. A. McClatchey et al, 1973, AFCRL Atmospheric Absorption Line Parameter Compilation, AFGL-TR-73-0096, Air Force Geophysics Laboratory, Hanscom AFB, MA.

2. Self-to-foreign broadening coefficients (B) experimentally determined for each laser line frequency,[1] as shown in table 2, have been used instead of the canonical value of 5.0.

TABLE 2. SELF-TO-FOREIGN BROADENING COEFFICIENTS USED IN THE LINE-BY-LINE CALCULATIONS

Laser Line	Frequency (cm^{-1})	B
$P_1(7)$	3644.1454	5.00
$P_2(5)$	3577.5002	6.30
$P_2(6)$	3531.1747	3.91
$P_2(7)$	3483.6522	8.20
$P_2(8)$	3434.9994	5.00

3. The modified Lorentz profile of reference 1 (or a Voigt derived from it) has been used, with η taken as 1.88, which is the optimum value determined in reference 1 for water vapor lines in the HF laser region.

Comparisons of calculated coefficients with the experimental data presented above are shown in figures 17 through 20, and the computed coefficients for line $P_2(6)$ (used to calibrate the data) are given in figure 21. Previous experimental work[1] comparing long-path absorption measurements with line-by-line values based on the 1978 AFGL tape indicated that agreement could be obtained only if the modified line profile of reference 1 was used and if the tape was modified by replacing the tabulated water vapor parameters with those evaluated by Flaud and Camy-Peyret.[4] The 1980 version of the AFGL atlas, used in the current computations, has been updated to incorporate the Flaud, Camy-Peyret values. As can be seen from figures 17 through 20, this version of the tape, when used with the modified line profile, does an exceptionally

---

[1]Wendell R. Watkins et al, 1978, Water Vapor Absorption Coefficients At HF Laser Wavelengths, Part I: Atmospheric Conditions Corresponding to Altitudes up to 7 km, ASL-TR-0007, US Army Atmospheric Sciences Laboratory, White Sands Missile Range, NM.

[4]J. M. Flaud and C. Camy-Peyret, 1975, "Vibration-Rotation Intensities in H_2O - Type Molecules, Application to the $2\nu_2$, ν_1 and ν_3 Bands of $H_2{}^{16}O$," J Mol Spectry, 55:278.

good job of predicting the observed coefficients at higher total pressures, although some minor deviations occur at low pressures.

Of the lines observed, $P_2(5)$ and $P_2(7)$ show exceptional agreement with calculated values while $P_1(7)$ and $P_2(8)$ show minor discrepancies. The deviations observed for laser line $P_2(8)$ may simply be a result of the high background "noise" level observed in the spectrophone system when operating on this line. The discrepancies observed for laser line $P_1(7)$, cannot be explained in terms of experimental uncertainties because the coefficients for this line are large and are several orders of magnitude above the observed noise level of the system. However, the systematic underprediction of the coefficients by the line-by-line calculations is the same type of behavior observed elsewhere[1] in comparing this type of calculation with long-path absorption data. Because the calculations agree with the data at high pressures while overpredicting the absorption at lower pressures, the problem may be associated with two weak water vapor lines in the tabulation* which are predicted to be in almost exact coincidence with the laser frequency (3644.1454 cm^{-1}). At higher pressures, these lines would broaden, decreasing their peak absorption and their contribution would be small compared to the wings of stronger adjacent lines. At lower pressures, however, the wings of adjacent lines would be diminished and the peaks of these weaker lines increased, so that they could have a significant effect upon the calculated coefficients. If these lines (or the laser line frequency) were shifted by as little as 0.0[illegible] cm^{-1}, much of this overprediction could be eliminated.

Because the observed data appear to follow the simplified relationship

$$K(\nu) = A(\nu)P_t^{\alpha(\nu)}P_s \qquad (5)$$

calculations of absorption coefficients at low water vapor pressures can most easily be determined using this function in conjunction with the parameters $A(\nu)$ and $\alpha(\nu)$ listed in table 3. However, the parameters of table 3 are those appropriate for ambient temperature, at which the data were collected. For actual upper altitude simulations in which the temperature is lower,

---

[1]Wendell R. Watkins et al, 1978, Water Vapor Absorption Coefficients At HF Laser Wavelengths, Part I: Atmospheric Conditions Corresponding to Altitudes up to 7 km, ASL-TR-0007, US Army Atmospheric Sciences Laboratory, White Sands Missile Range, NM.

*In the notation $J'_{\kappa a',\kappa c'} - J''_{\kappa a'',\kappa c''}$ these lines are: $11_{5,7} - 10_{7,4}$(V = 001 - 000) at 3644.1413 cm^{-1} and $5_{4,1} - 4_{1,4}$(V = 020 - 000) at 3644.1480 cm^{-1}.

line-by-line calculations should either be used directly or be used to generate appropriate values of $A(\nu)$ and $\alpha(\nu)$.

TABLE 3. PARAMETERS $A(\nu)$ AND $\alpha(\nu)$ DETERMINED IN FITTING THE EXPERIMENTAL DATA TO $K(\nu) = A(\nu)\, P_t^{\alpha(\nu)} P_s$

Laser Line	$A(\nu)$	$\alpha(\nu)$
$P_1(7)$	1.3983E-02	0.78473
$P_2(5)$	1.6090E-02	0.81872
$P_2(6)$	1.0039E-02	0.87183
$P_2(7)$	1.4339E-02	0.86551

CONCLUSIONS

Absorption coefficients were measured at HF laser lines using low water vapor pressures and total pressures ranging from 125 to 700 torr. These measurements were made using a unique differential photoacoustic system which allowed coefficients to be determined to 5×10^{-3} km^{-1}. The results of these measurements were found to be well represented by a function of the form

$$K(\nu) = A(\nu) P_t^{\alpha(\nu)} P_s \qquad (6)$$

where $A(\nu)$ and $\alpha(\nu)$ were determined for each laser frequency. Comparisons of these data with calculated values based on a modified Lorentz profile, with an augmented line wing, and spectroscopic parameters tabulated in the 1980 AFGL atmospheric absorption line compilation, showed good agreement for all lines at high pressures ($\approx$700 torr), with some discrepancies appearing at lower pressures. The discrepancies were most significant at HF laser line $P_1(7)$; however, these can be explained in terms of a possible mispositioning in the tabulation of a pair of water vapor lines, which are currently within 0.004 cm^{-1} of the laser frequency.

In general, the current data appear to support previous findings[1] that water vapor lines exhibit augmented wing absorption relative to the standard Lorentz profile and that agreement with experimental observations can be obtained if updated parameters are used in conjunction with a profile of the form presented in reference 1.

---

[1]Wendell R. Watkins et al, 1978, Water Vapor Absorption Coefficients At HF Laser Wavelengths, Part I: Atmospheric Conditions Corresponding to Altitudes up to 7 km, ASL-TR-0007, US Army Atmospheric Sciences Laboratory, White Sands Missile Range, NM.

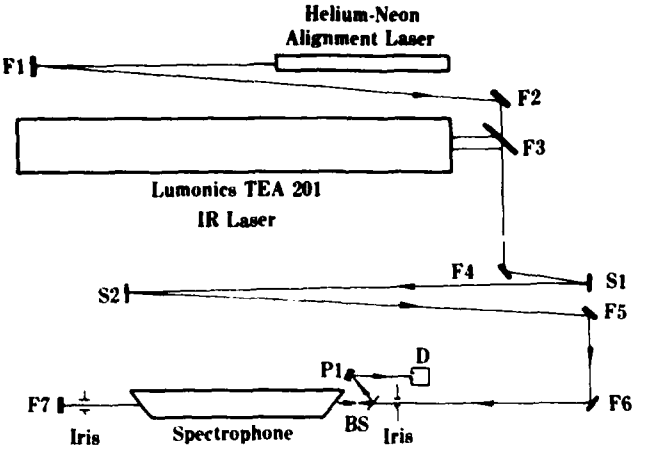

Figure 1. Schematic of the optical layout used for spectrophone absorption measurement.

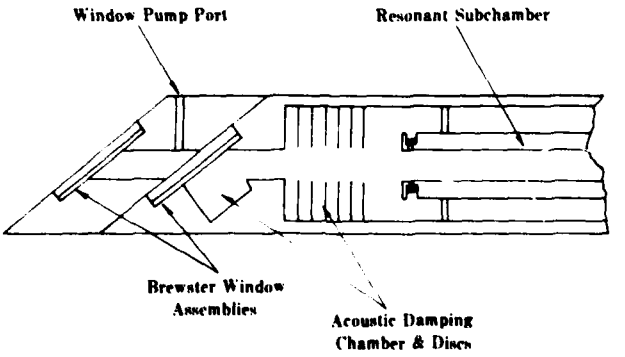

Figure 2. Schematic of the spectrophone chamber showing the window assemblies and the resonant subchamber.

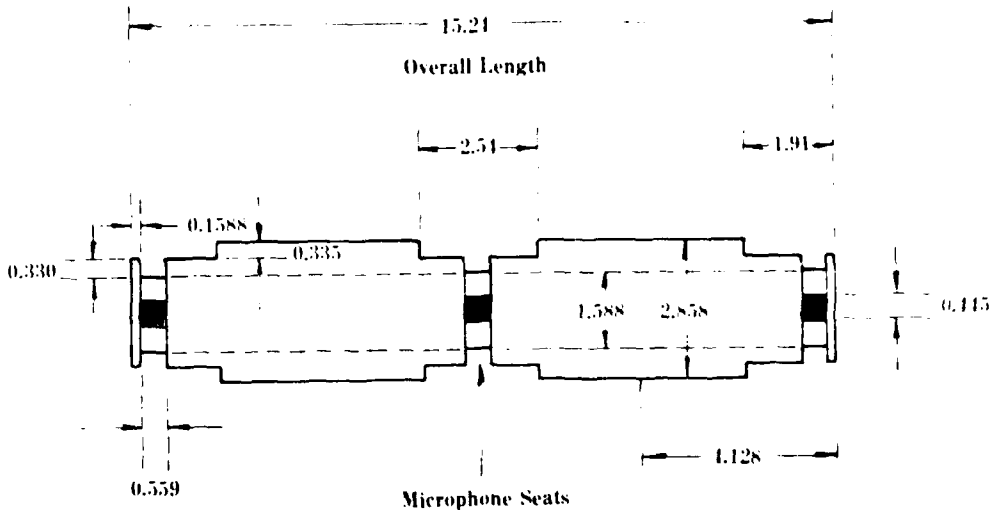

Figure 3. Schematic of the differential resonant subchamber employing 12 electret microphones.

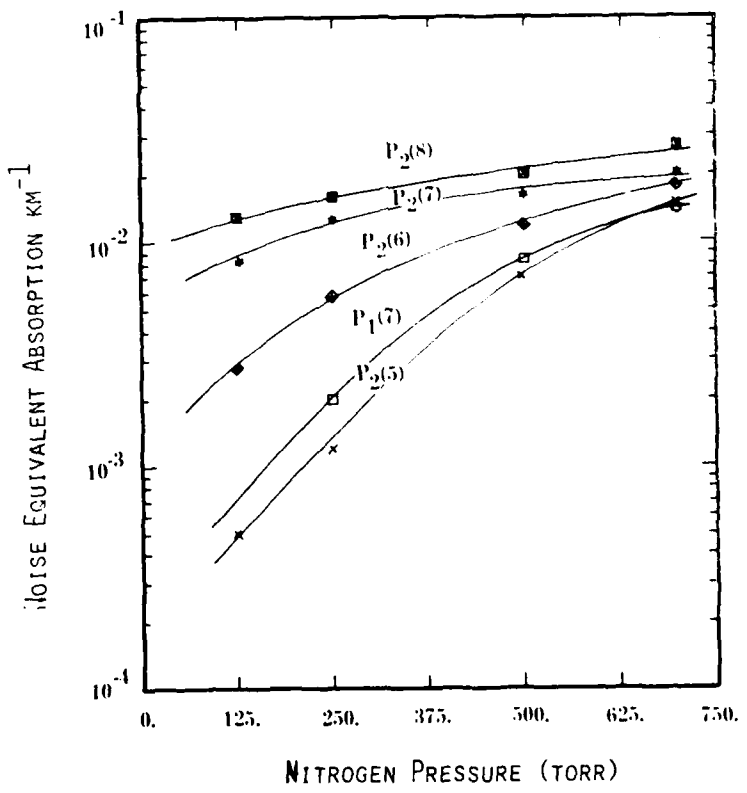

Figure 4. Background "noise" level for the various laser lines as a function of nitrogen pressure.

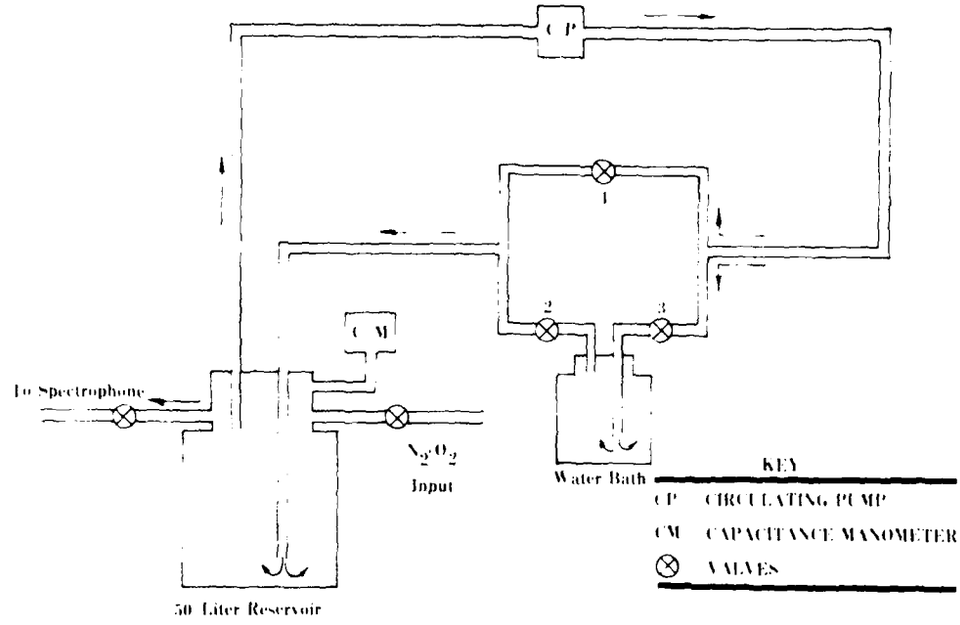

Figure 5. Reservoir system for generating low water vapor content gas mixtures.

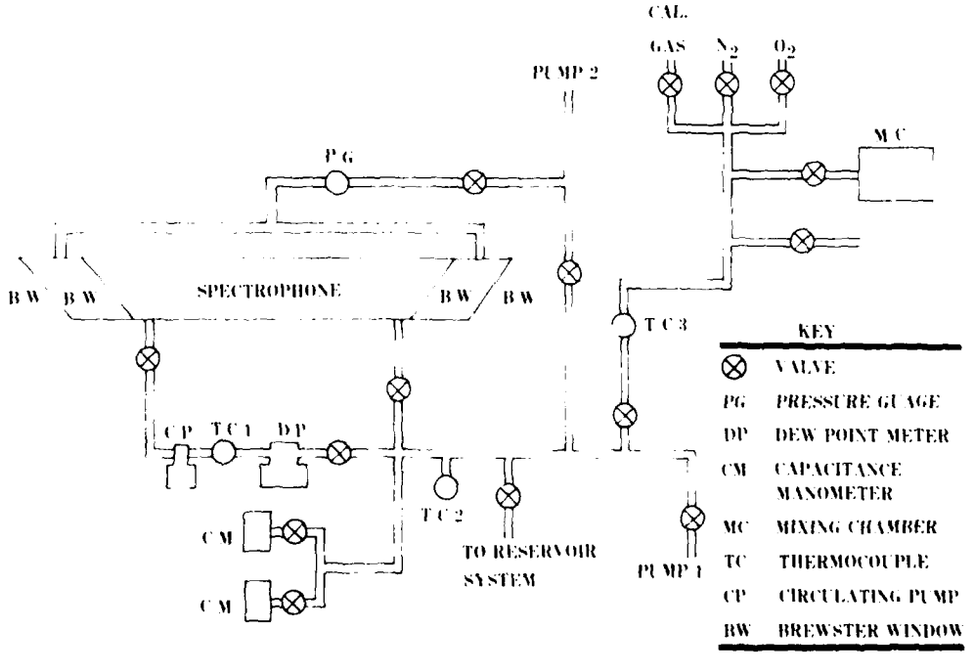

Figure 6. Schematic of the spectrophone fill and circulation systems.

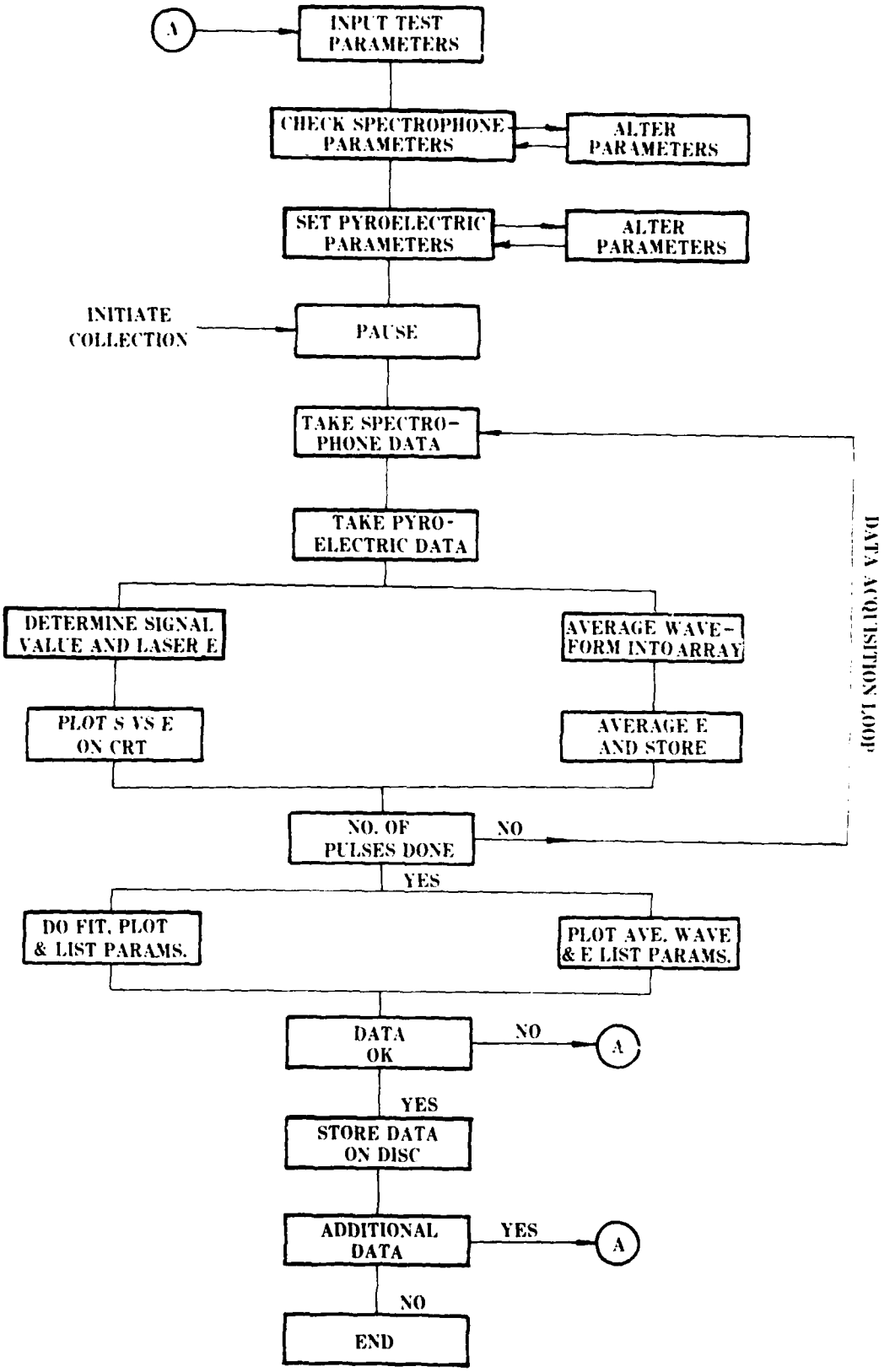

Figure 7. Logic flow chart for data acquisition software.

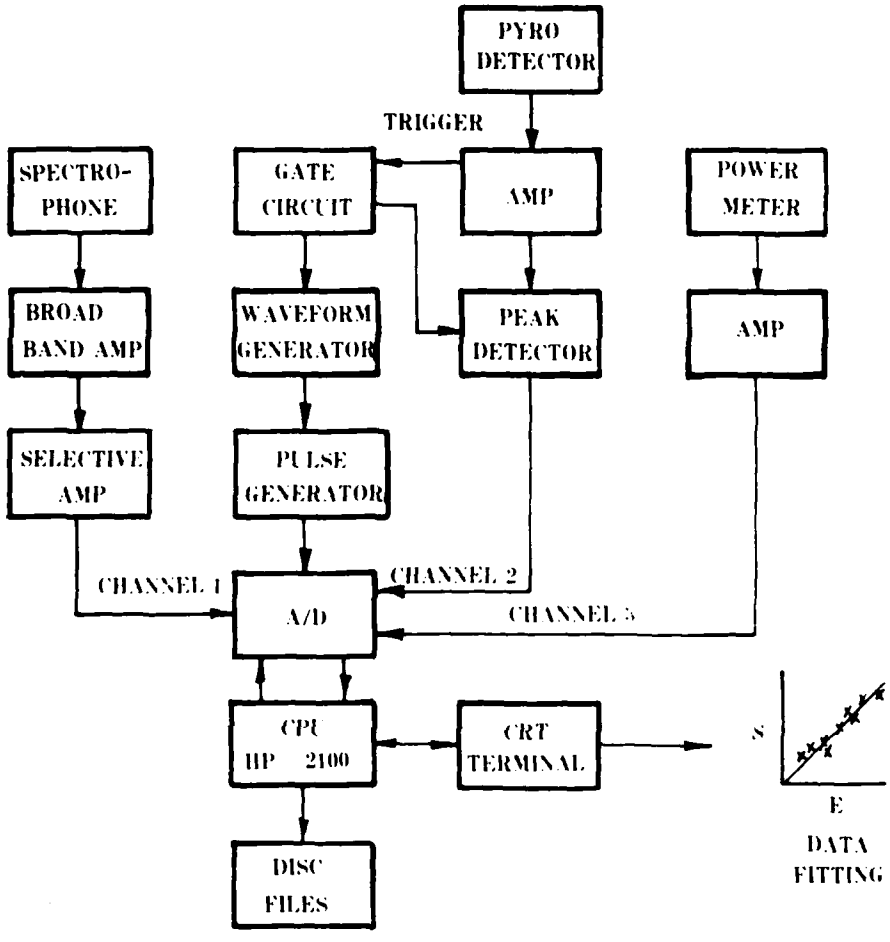

Figure 8. Electronic systems used for data acquisition and storage.

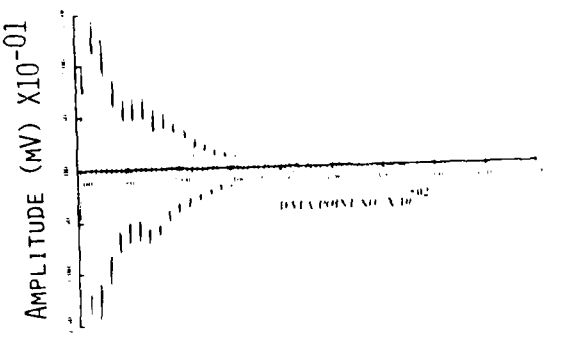

Figure 9. Typical output waveform obtained from the resonant spectrophone with a pulsed laser source.

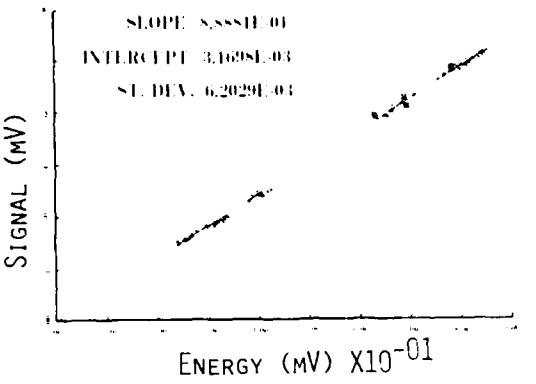

Figure 10. Signal versus power and linear least squares fit with a spectrophone fill giving an absorption coefficient of 1.5 km^{-1}.

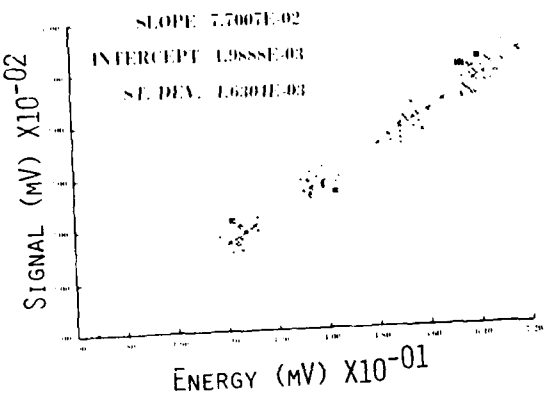

Figure 11. Signal versus power and linear least squares fit with a spectrophone fill giving an absorption coefficient of 0.13 km^{-1}.

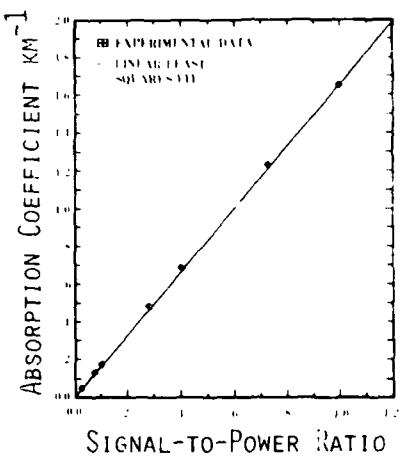

Figure 12. Typical spectrophone calibration curve obtained using HF laser line $P_2(6)$.

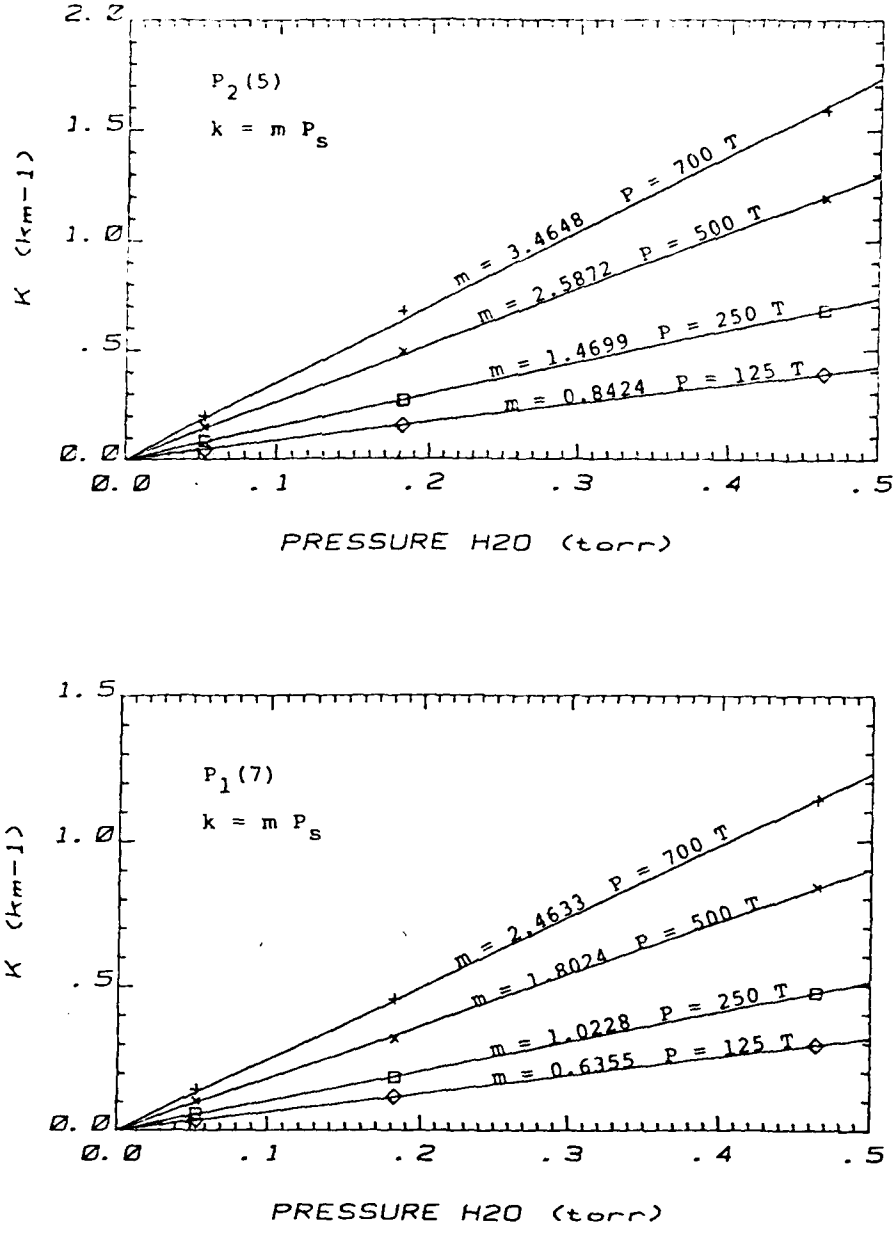

Figure 13. Linear least squares fits to observed absorption coefficients for HF laser lines $P_2(5)$ and $P_1(7)$ at 125, 250, 500, and 700 torr total pressure.

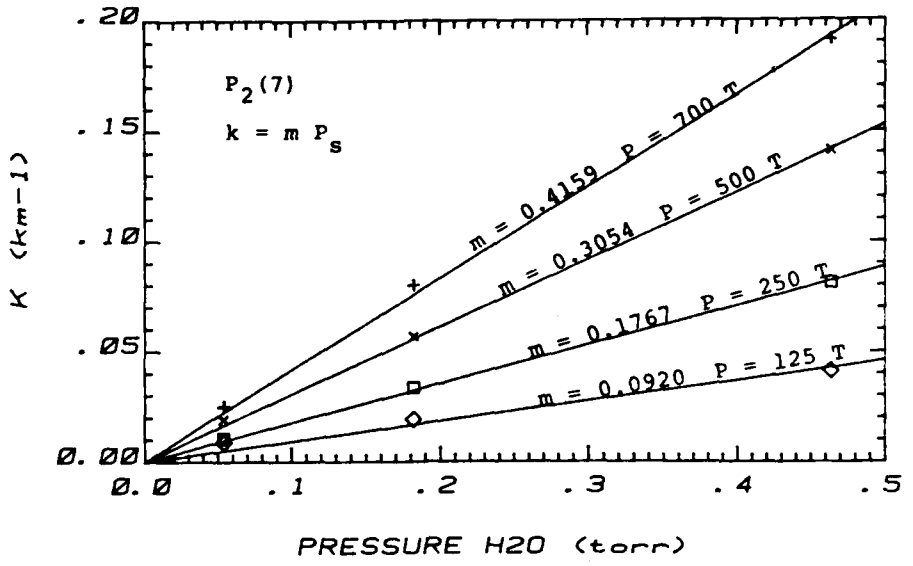

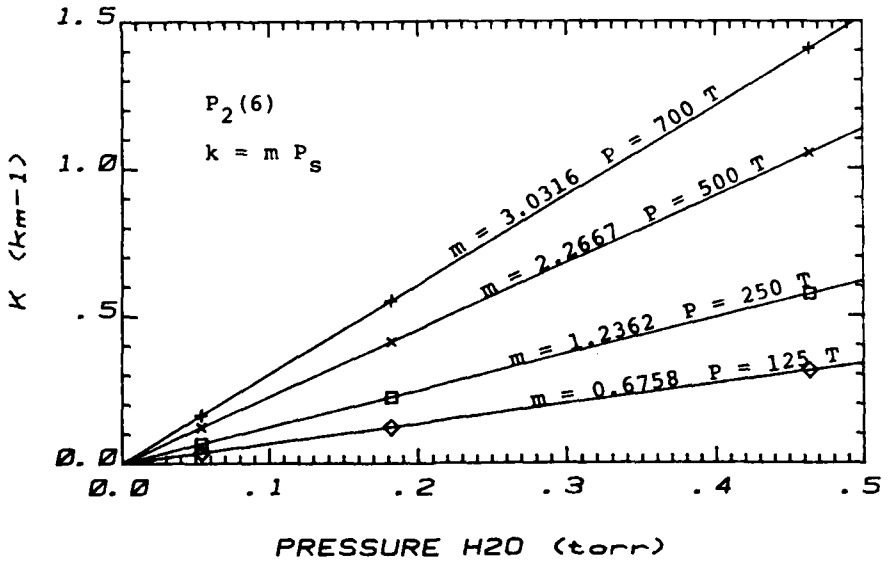

Figure 14. Linear least squares fits to observed absorption coefficients for HF laser lines $P_2(7)$ and $P_2(6)$ at 125, 250, 500, and 700 torr total pressure.

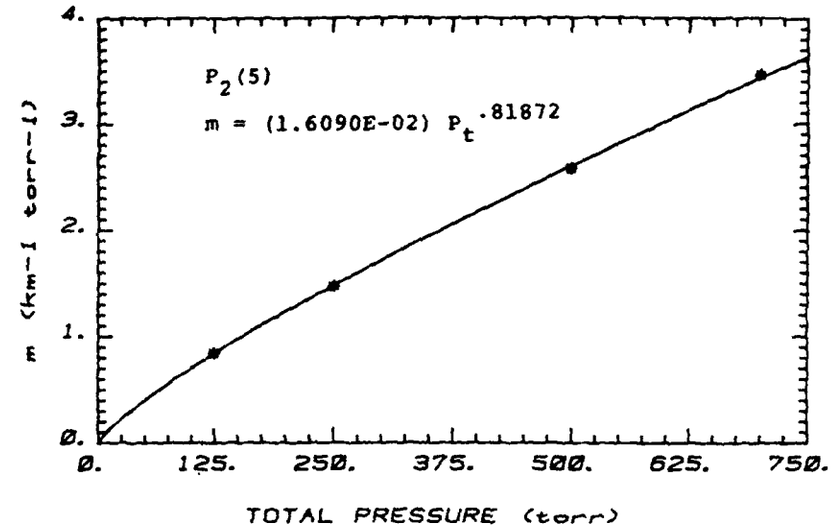

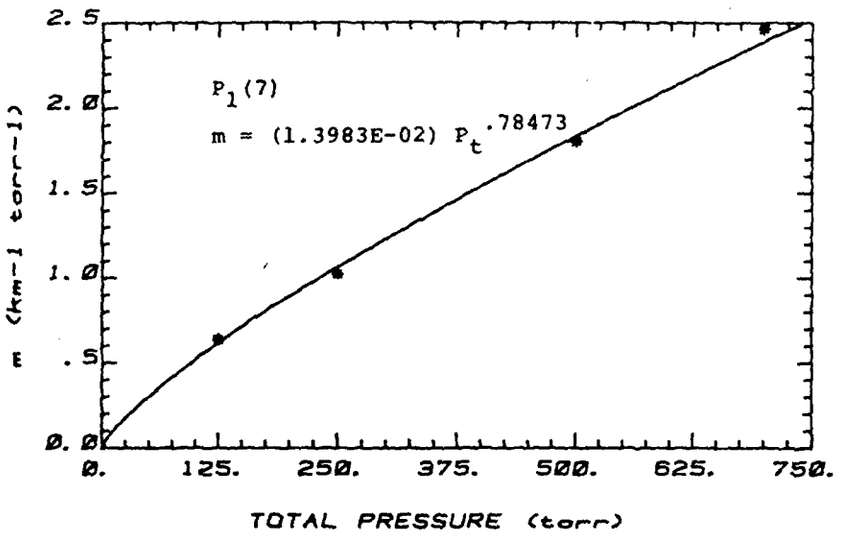

Figure 15. Least squares fits to the differential absorption coefficients of HF laser lines $P_1(7)$ and $P_2(5)$ as a function of total pressure.

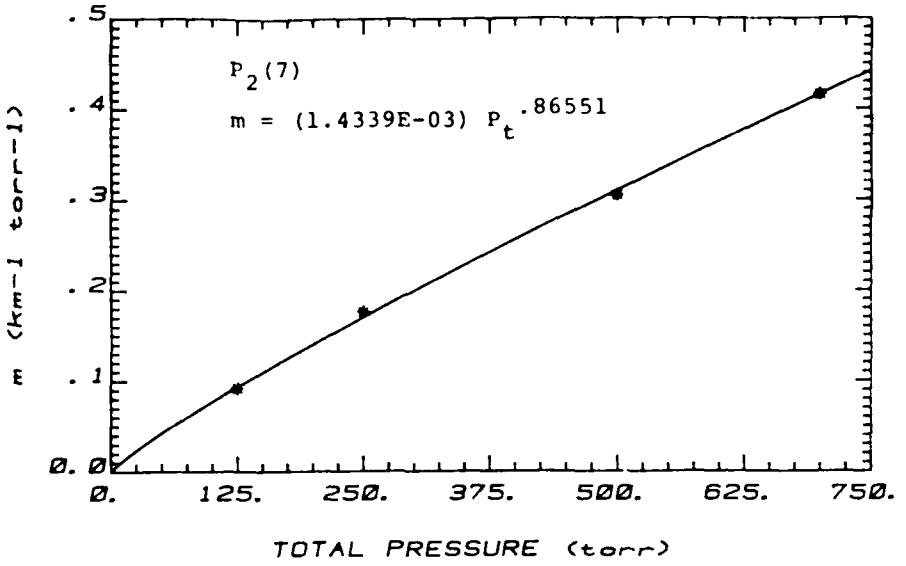

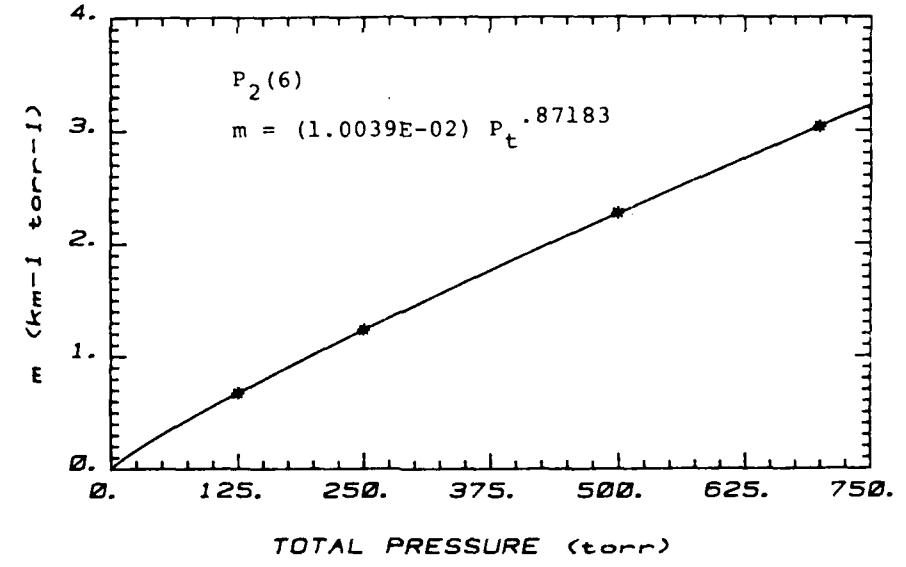

Figure 16. Least squares fits to the differential absorption coefficients of HF laser lines $P_2(6)$ and $P_2(7)$ as a function of total pressure.

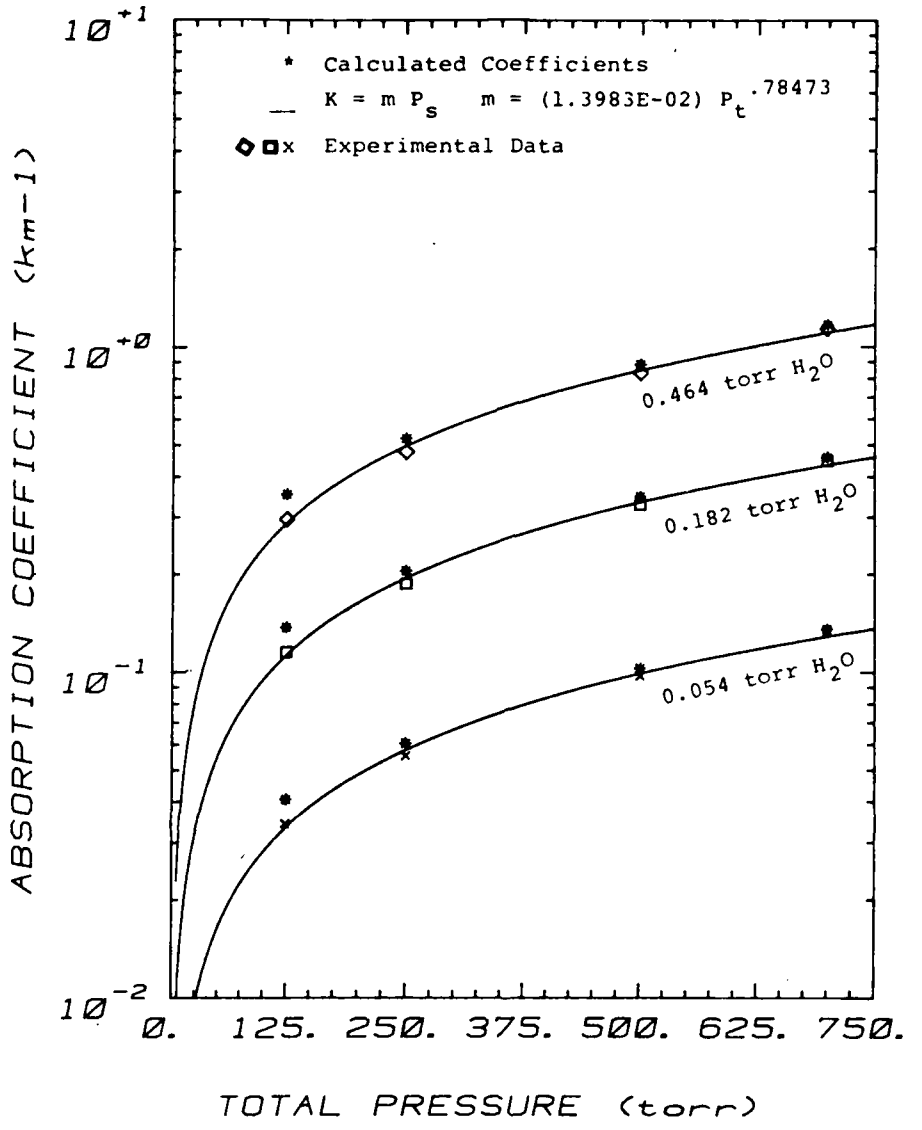

Figure 17. Observed absorption coefficients for laser line $P_1(7)$ compared to those calculated using line-by-line procedures.

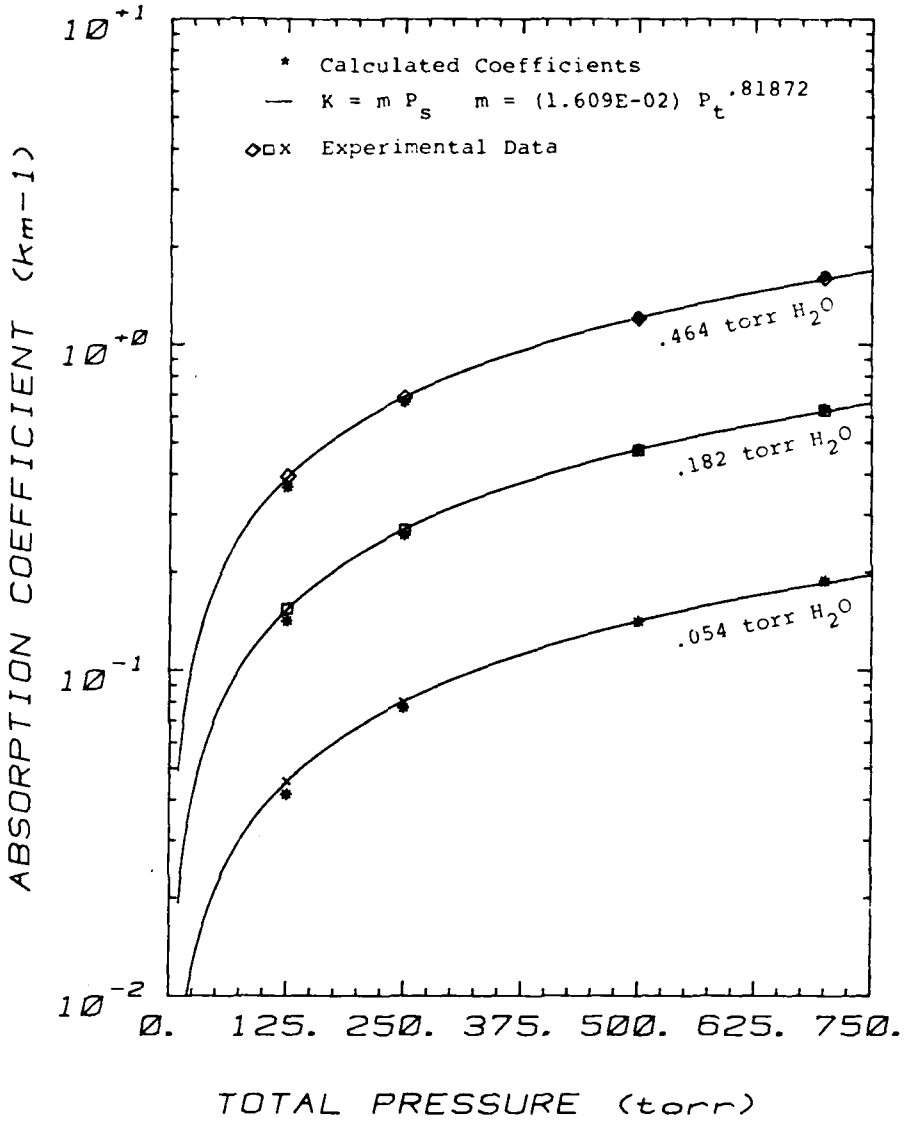

Figure 18. Observed absorption coefficients for laser line $P_2(5)$ compared to those calculated using line-by-line procedures.

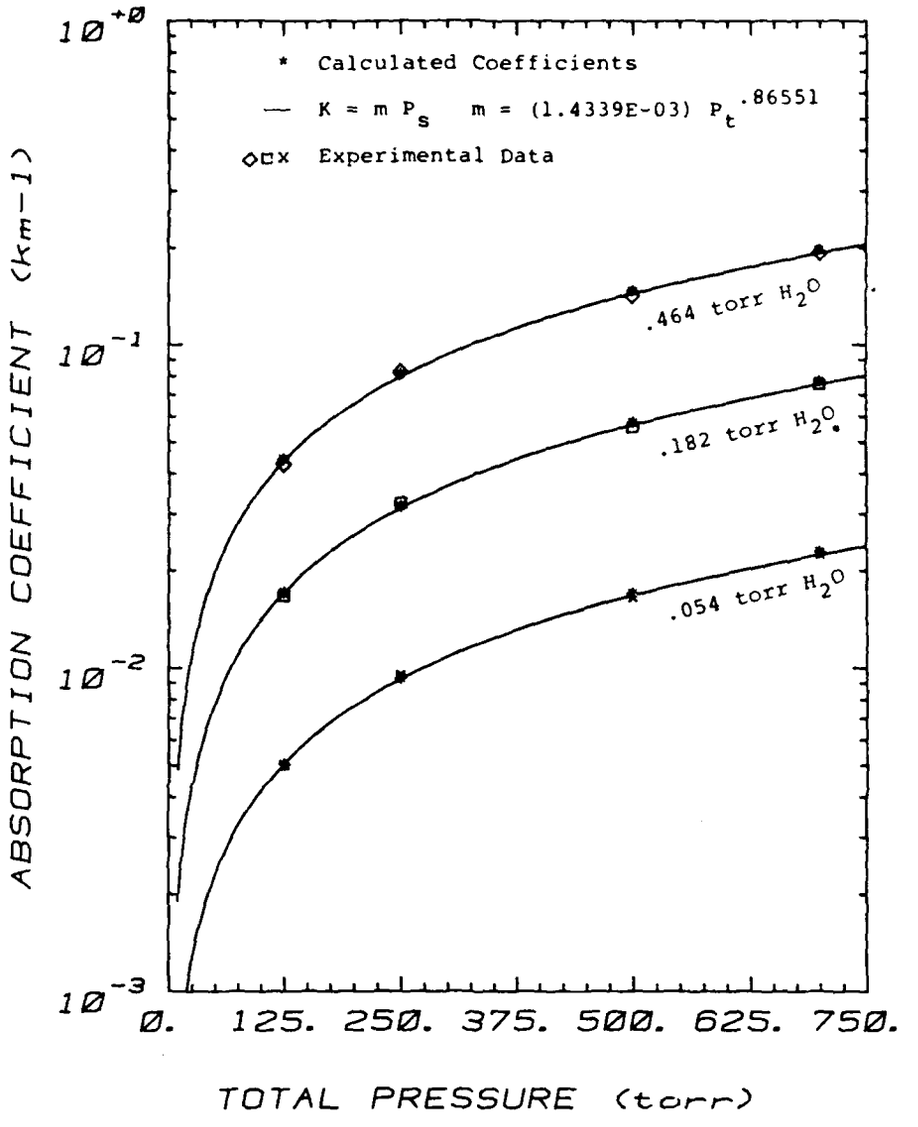

Figure 19. Observed absorption coefficients for laser line $P_2(7)$ compared to those calculated using line-by-line procedures.

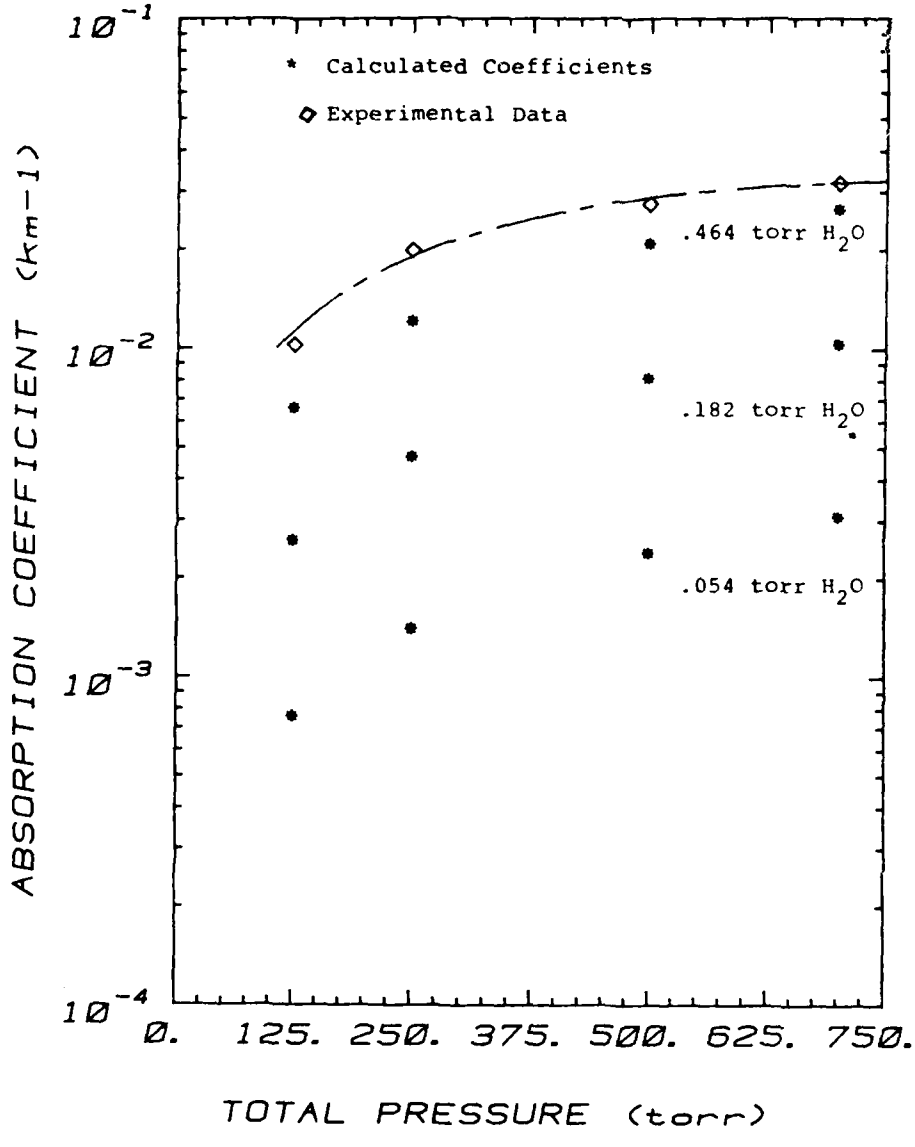

Figure 20. Observed absorption coefficients for laser line $P_2(8)$ compared to those calculated using line-by-line procedures.

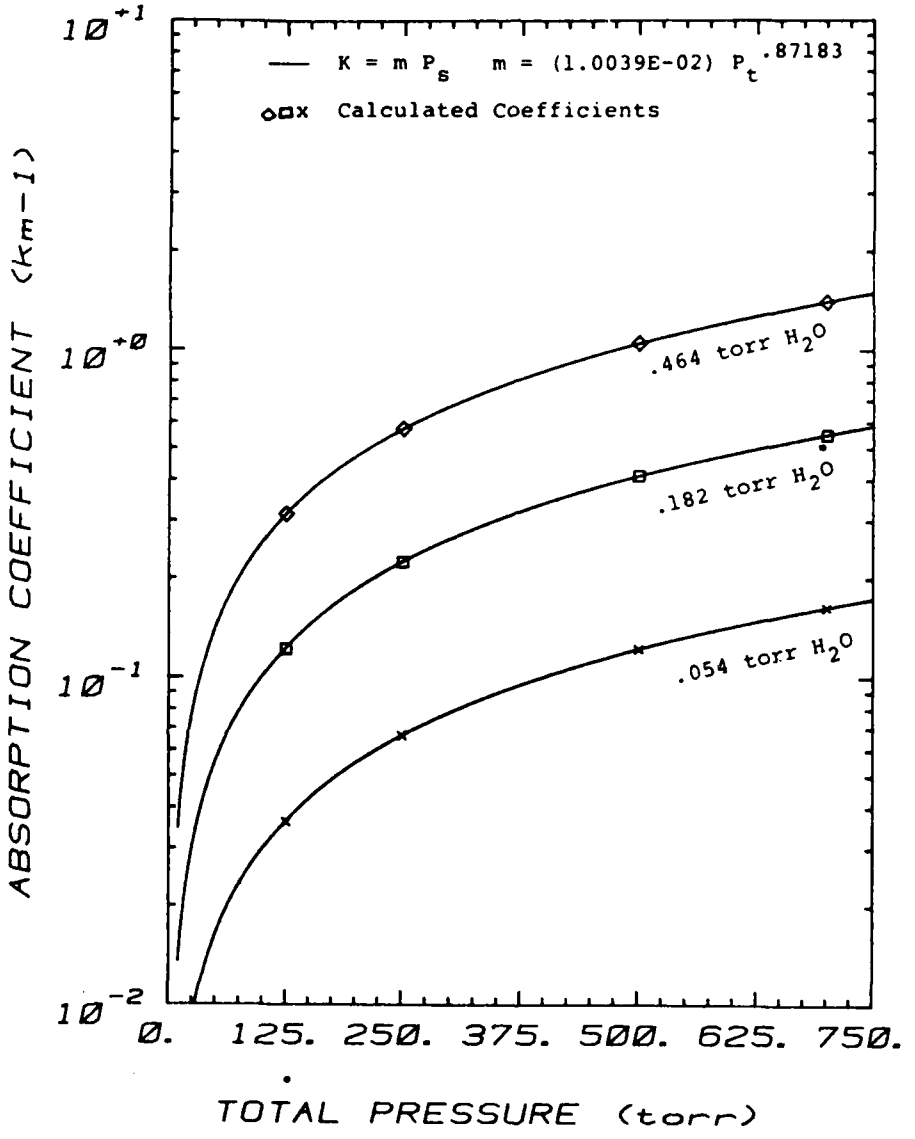

Figure 21. Calculated coefficients for laser line $P_2(6)$ used for calibration of the spectrophone data.

APPENDIX A

BACKGROUND

For a typical midlatitude summer atmospheric profile the water vapor pressure at 10 km is on the order of 50 to 60 mtorr, while the total pressure is approximately 200 torr. Under these circumstances, the absorption coefficients for HF laser lines vary from about 10^{-1} per kilometer to less than 10^{-3} per kilometer. If these coefficients are to be determined from transmission measurements for which the transmission (τ) is related to the absorption coefficient (K) through Beer's law, the errors in K are given by

$$(\Delta K/K) = [1/\ln(\tau)](\Delta\tau/\tau) \tag{A-1}$$

where $(\Delta\tau/\tau)$ represents the accuracy of the transmission measurement. Consequently, even with a 1.5 km measurement path and a 1 percent measurement accuracy $(\Delta\tau/\tau)$, the errors incurred in the determination of K are: 6.7 percent for $K \approx 0.1$ km^{-1}, 67 percent for $K \approx 0.01$ km^{-1}, and 670 percent for $K \approx 0.001$ km^{-1}. It is obvious from these figures that measurement of transmission is not the best method for use in determining small absorption coefficients, and that an alternate approach which evaluates K directly is required.

Photoacoustic detection, which exhibits these desired characteristics, is the approach chosen for the present program. In effect, this type of detection measures the pressure rise taking place in an enclosed sample of gas as a result of the absorption of radiation and the subsequent transfer of this absorbed energy to kinetic energy through collisional deactivation. To determine the pressure response (p) of a system due to the addition of heat (H) through absorption of radiation, one must solve the standard wave equation

$$\nabla^2 p - \frac{1}{C_o^2}\frac{\partial^2 p}{\partial t^2} = -\frac{(\gamma - 1)}{c_o^2}\frac{\partial H}{\partial t} \tag{A-2}$$

where c_o is the velocity of sound and γ is the ratio of specific heats (C_p/C_v). As shown by Rosencwaig,[1] the easiest way to solve this equation is to take its Fourier transform and find solutions of the resultant equation in terms of the normal modes of the system (that is, the solutions of the corresponding homogeneous wave equation).

---

[1]Allan Rosencwaig, 1980, Photo-acoustics and Photo-acoustic Spectroscopy, John Wiley & Sons, Inc., New York.

If this is done for an open cylindrical chamber of radius a and length ℓ, the normal modes are found to be

$$P_j = \cos(m\phi)[A\, J_m(k_r r)][B\, \sin(k_z z)] \qquad \text{(A-3)}$$

where J_m is the Bessel function of the first kind, Z the axial dimension in the cavity, r the radial dimension and

$$k_z = \frac{\pi}{\ell} n_z \qquad n_z = 1,2,3...$$

$$k_r = \frac{\pi}{a} \alpha_{mn}$$

where α_{mn} is defined by

$$J'_m(\pi\alpha_{mn}) = 0 \ .$$

The frequencies of the normal modes defined by the integers m, n, and n_z are then given by

$$\omega_j = C_o(k_r^2 + k_z^2)^{1/2} \qquad \text{(A-4)}$$

and the general solution for the pressure response of the photoacoustic system is

$$p(r,\omega) = \sum_j A_j(\omega) p_j(r) \qquad \text{(A-5)}$$

This represents the spectrum of the resultant pressure response, written in terms of the spatially dependent normal mode structures $p_j(r)$ and corresponding amplitude functions $A_j(\omega)$ defining the frequency dependence of the j^{th} mode. By substituting equation (14) into the transformed wave equation one may show that the complex amplitudes are given by

$$A_j(\omega) = -i\,\omega \frac{[K(\gamma - 1)/V_c] \int p^*_j\, I\, dv}{(\omega_g^2 - \omega^2)} \qquad \text{(A-6)}$$

where K is the absorption coefficient, I the optical beam intensity, and V_c the chamber volume. The numerator of this equation represents the coupling between the beam and the normal mode j while the denominator represents the resonant conditions, if any, which exist in the photoacoustic chamber. The fact that this amplitude tends to infinity as μ tends to μ_j is the result of ignoring disipative forces acting on the pressure wave in the chamber. These effects can be added as a perturbation, modifying the above expression through the addition of a quality factor Q_j for each mode. This gives

$$A_j(\omega) = -i\ \omega \frac{[K(\gamma - 1)/V_c] \int P^*_j\ I\ dv}{(\omega_j^2 - \omega^2) - i(\omega\omega_j/Q_j)} \qquad \text{(A-7)}$$

The moduli squared of these complex amplitude functions represent the profiles for the various modes in the Weiner or power spectrum. For a nonresonant system and a spatially constant input beam, the only mode present is the DC or zero frequency mode for which

$$|A_o(\omega)|^2 = \frac{[K(\gamma - 1)W1/V_c]^2}{w^2 + (1/\tau_o)^2} \qquad \text{(A-8)}$$

where τ_o is the damping time constant arising from heat conduction to the walls of the chamber and W is now the input power (watts). Therefore, if a nonresonant system is illuminated with a laser of power W and the pressure is allowed to reach its maximum value, this maximum will be proportional to

$$P_{max}\ \alpha[K1(\gamma - 1)W/V_c]\tau_o \qquad \text{(A-9)}$$

Since the amplitude of this nonresonant pressure rise is directly proportional to the absorption coefficient (K) and the input power (W), a photoacoustic system could be operated in this mode, with K being determined by monitoring the pressure rise resulting from a given input power. From a practical point of view, however, this is not an ideal operating mode, because the pressure sensor and associated electronics must operate at DC and are consequently susceptible to 1/f noise in the electronics and long term drifts in the system. If one attempts to chop the input beam so that synchronous detection can be used, extremely low frequencies must be used because the pressure response drops off as $1/\omega$.

To avoid these problems, a photoacoustic detector can be set up as an acoustically resonant system and operated at its fundamental resonant frequency. Under these circumstances, the power spectrum amplitude is given by[1]

$$|A_1(\omega)|^2 = \frac{\omega^2 [K1(\gamma - 1)W/V_c]^2}{(\omega_1^2 - \omega^2)^2 + (\omega\omega_1/Q_1)^2} \qquad \text{(A-10)}$$

If the system is driven at resonance ($\omega = \omega_1$), the pressure response will be proportional to

$$p_{max} \propto [K1(\gamma - 1)W/V_c](Q_1/\omega_1) \qquad \text{(A-11)}$$

This exhibits the same dependence on K and W as the nonresonant case. Consequently, absorption coefficients can again be evaluated by simply measuring the pressure response of the system for a given input power. Unlike the nonresonant case, however, this response has a (Q/ω) dependence, so that the $(1/\omega)$ falloff can be counteracted by using a high Q cavity. In addition, use of a high Q cavity also allows for narrow bandpass detection of the resultant signals, substantially reducing the background noise.

In the present investigation only a pulsed HF laser was available. Although the same general expressions apply when using a pulsed source, the gain normally associated with a high Q cavity will not be realized unless the laser repetition rate is short compared to (Q/ω). Unfortunately, this is normally not the case so that what is obtained as output in the time domain from a pulse-operated system is a damped pressure response with a peak proportional to

$$\frac{K\ 1(\gamma - 1)W}{V_c} \qquad \text{(A-12)}$$

and a damping envelope given by e^{-t/τ_o} for the nonresonant case and $e^{-t\omega_1 Q_1}$ for a resonant case. However, it is still advantageous to use a resonant system, since: operation at higher frequencies avoids the 1/f noise associated with the pressure transducer and electronics; narrow bandpass amplification, which eliminates much of the background noise can be used; and small, highly sensitive microphones can be used instead of larger volume, less sensitive capacitance manometers.

---

[1]Allan Rosencwaig, 1980, Photo-acoustics and Photo-acoustic Spectroscopy, John Wiley & Sons, Inc., New York.

ELECTRO-OPTICS DISTRIBUTION LIST

Commander
US Army Aviation School
Fort Rucker, AL 36362

Commander
US Army Aviation Center
ATTN: ATZQ-D-MA (Mr. Oliver N. Heath)
Fort Rucker, AL 36362

Commander
US Army Aviation Center
ATTN: ATZQ-D-MS (Mr. Donald Wagner)
Fort Rucker, AL 36362

NASA/Marshall Space Flight Center
ATTN: ES-83 (Otha H. Vaughan, Jr.)
Huntsville, AL 35812

NASA/Marshall Space Flight Center
Atmospheric Sciences Division
ATTN: Code ES-81 (Dr. William W. Vaughan)
Huntsville, AL 35812

Nichols Research Corporation
ATTN: Dr. Lary W. Pinkley
4040 South Memorial Parkway
Huntsville, AL 35802

John M. Hobbie
c/o Kentron International
2003 Byrd Spring Road
Huntsville, AL 35802

Mr. Ray Baker
Lockheed-Missile & Space Company
4800 Bradford Blvd
Huntsville, AL 35807

Commander
US Army Missile Command
ATTN: DRSMI-OG (Mr. Donald R. Peterson)
Redstone Arsenal, AL 35809

Commander
US Army Missile Command
ATTN: DRSMI-OGA (Dr. Bruce W. Fowler)
Redstone Arsenal, AL 35809

Commander
US Army Missile Command
ATTN: DRSMI-REL (Dr. George Emmons)
Redstone Arsenal, AL 35809

Commander
US Army Missile Command
ATTN: DRSMI-REO (Huey F. Anderson)
Redstone Arsenal, AL 35809

Commander
US Army Missile Command
ATTN: DRSMI-REO (Mr. Maxwell W. Harper)
Redstone Arsenal, AL 35809

Commander
US Army Missile Command
ATTN: DRSMI-REO (Mr. Gene Widenhofer)
Redstone Arsenal, AL 35809

Commander
US Army Missile Command
ATTN: DRSMI-RHC (Dr. Julius Q. Lilly)
Redstone Arsenal, AL 35809

Commander
US Army Missile Command
Redstone Scientific Information Center
ATTN: DRSMI-RPRD (Documents Section)
Redstone Arsenal, AL 35809

Commander
US Army Missile Command
ATTN: DRSMI-RRA (Dr. Oskar Essenwanger)
Redstone Arsenal, AL 35809

Commander
US Army Missile Command
ATTN: DRSMI-RRO (Mr. Charles Christensen)
Redstone Arsenal, AL 35809

Commander
US Army Missile Command
ATTN: DRSMI-RRO (Dr. George A. Tanton)
Redstone Arsenal, AL 35809

Commander
US Army Communications Command
ATTN: CC-OPS-PP
Fort Huachuca, AZ 85613

Commander
US Army Intelligence Center & School
ATTN: ATSI-CD-CS (Mr. Richard G. Cundy)
Fort Huachuca, AZ 85613

Commander
US Army Intelligence Center & School
ATTN: ATSI-CD-MD (Mr. Harry Wilder)
Fort Huachuca, AZ 85613

Commander
US Army Intelligence Center & School
ATTN: ATSI-CS-C (2LT Coffman)
Fort Huachuca, AZ 85613

Commander
US Army Yuma Proving Ground
ATTN: STEYP-MSA-TL
Bldg 2105
Yuma, AZ 85364

Northrop Corporation
Electro-Mechanical Division
ATTN: Dr. Richard D. Tooley
500 East Orangethorpe Avenue
Anaheim, CA 92801

Commander
Naval Weapons Center
ATTN: Code 3918 (Dr. Alexis Shlanta)
China Lake, CA 93555

Hughes Helicopters
Army Advanced Attack Helicopter Weapons
ATTN: Mr. Charles R. Hill
Centinela and Teale Streets
Bldg 305, MS T-73A
Culter City, CA 90230

Commander
US Army Combat Developments
Experimentation Command
ATTN: ATEC-PL-M (Mr. Gary G. Love)
Fort Ord, CA 93941

SRI International
ATTN: K2060/Dr. Edward E. Uthe
333 Ravenswood Avenue
Menlo Park, CA 94025

SRI International
ATTN: Mr. J. E. Van der Laan
333 Ravenswood Avenue
Menlo Park, CA 94025

Joane May
Naval Environmental Prediction
Research Facility (NEPRF)
ATTN: Library
Monterey, CA 93940

Sylvania Systems Group,
Western Division
GTE Products Corporation
ATTN: Technical Reports Library
P.O. Box 205
Mountain View, CA 94042

Sylvania Systems Group
Western Division
GTE Products Corporation
ATTN: Mr. Lee W. Carrier
P.O. Box 188
Mountain View, CA 94042

Pacific Missile Test Center
Geophysics Division
ATTN: Code 3250-3 (R. de Violini)
Point Mugu, CA 93042

Pacific Missile Test Center
Geophysics Division
ATTN: Code 3253 (Terry E. Battalino)
Point Mugu, CA 93042

Effects Technology Inc.
ATTN: Mr. John D. Carlyle
5383 Hollister Avenue
Santa Barbara, CA 93111

Commander
Naval Ocean Systems Center
ATTN: Code 532 (Dr. Juergen Richter)
San Diego, CA 92152

Commander
Naval Ocean Systems Center
ATTN: Code 5322 (Mr. Herbert G. Hughes)
San Diego, CA 92152

Commander
Naval Ocean Systems Center
ATTN: Code 4473 (Tech Library)
San Diego, CA 92152

The RAND Corporation
ATTN: Ralph Huschke
1700 Main Street
Santa Monica, CA 90406

Particle Measuring Systems, Inc.
ATTN: Dr. Robert G. Knollenberg
1855 South 57th Court
Boulder, CO 80301

US Department of Commerce
National Oceanic and Atmospheric Admin
Environmental Research Laboratories
ATTN: Library, R-51, Technical Reports
325 Broadway
Boulder, CO 80303

US Department of Commerce
National Oceanic and Atmospheric Admin
Environmental Research Laboratories
ATTN: R45X3 (Dr. Vernon E. Derr)
Boulder, CO 80303

US Department of Commerce
National Telecommunications and
Information Administration
Institute for Telecommunication Sciences
ATTN: Code 1-3426 (Dr. Hans J. Liebe)
Boulder, CO 80303

AFATL/DLODL
Technical Library
Eglin AFB, FL 32542

Commanding Officer
Naval Training Equipment Center
ATTN: Technical Information Center
Orlando, FL 32813

Georgia Institute of Technology
Engineering Experiment Station
ATTN: Dr. Robert W. McMillan
Atlanta, GA 30332

Georgia Institute of Technology
Engineering Experiment Station
ATTN: Dr. James C. Wiltse
Atlanta, GA 30332

Commandant
US Army Infantry Center
ATTN: ATSH-CD-MS-E (Mr. Robert McKenna)
Fort Benning, GA 31805

Commander
US Army Signal Center & Fort Gordon
ATTN: ATZHCD-CS
Fort Gordon, GA 30905

Commander
US Army Signal Center & Fort Gordon
ATTN: ATZHCD-O
Fort Gordon, GA 30905

USAFETAC/DNE
ATTN: Mr. Charles Glauber
Scott AFB, IL 62225

Commander
Air Weather Service
ATTN: AWS/DNDP (LTC Kit G. Cottrell)
Scott AFB, IL 62225

Commander
Air Weather Service
ATTN: AWS/DOOF (MAJ Robert Wright)
Scott AFB, IL 62225

Commander
US Army Combined Arms Center
& Ft. Leavenworth
ATTN: ATZLCA-CAA-Q (Mr. H. Kent Pickett)
Fort Leavenworth, KS 66027

Commander
US Army Combined Arms Center
& Ft. Leavenworth
ATTN: ATZLCA-SAN (Robert DeKinder, Jr.)
Fort Leavenworth, KS 66027

Commander
US Army Combined Arms Center
& Ft. Leavenworth
ATTN: ATZLCA-SAN (Mr. Kent I. Johnson)
Fort Leavenworth, KS 66027

Commander
US Army Combined Arms Center
& Ft. Leavenworth
ATTN: ATZLCA-WE (LTC Darrell Holland)
Fort Leavenworth, KS 66027

President
USAARENBD
ATTN: ATZK-AE-TA (Dr. Charles R. Leake)
Fort Knox, KY 40121

Commander
US Army Armor Center and Fort Knox
ATTN: ATZK-CD-MS
Fort Knox, KY 40121

Commander
US Army Armor Center and Fort Knox
ATTN: ATZK-CD-SD
Fort Knox, KY 40121

Aerodyne Research Inc.
ATTN: Dr. John F. Ebersole
Crosby Drive
Bedford, MA 01730

Commander
Air Force Geophysics Laboratory
ATTN: OPA (Dr. Robert W. Fenn)
Hanscom AFB, MA 01731

Commander
Air Force Geophysics Laboratory
ATTN: OPI (Dr. Robert A. McClatchey)
Hanscom AFB, MA 01731

Massachusetts Institute of Technology
Lincoln Laboratory
ATTN: Dr. T. J. Goblick, B-370
P.O. Box 73
Lexington, MA 02173

Massachusetts Institute of Technology
Lincoln Laboratory
ATTN: Dr. Michael Gruber
P.O. Box 73
Lexington, MA 02173

Raytheon Company
Equipment Division
ATTN: Dr. Charles M. Sonnenschein
430 Boston Post Road
Wayland, MA 01778

Commander
US Army Ballistic Research Laboratory/
ARRADCOM
ATTN: DRDAR-BLB (Mr. Richard McGee)
Aberdeen Proving Ground, MD 21005

Commander/Director
Chemical Systems Laboratory
US Army Armament Research
& Development Command
ATTN: DRDAR-CLB-PS (Dr. Edward Stuebing)
Aberdeen Proving Ground, MD 21010

Commander/Director
Chemical Systems Laboratory
US Army Armament Research
& Development Command
ATTN: DRDAR-CLB-PS (Mr. Joseph Vervier)
Aberdeen Proving Ground, MD 21010

Commander/Director
Chemical Systems Laboratory
US Army Armament Research
& Development Command
ATTN: DRDAR-CLY-A (Mr. Ronnald Pennsyle)
Aberdeen Proving Ground, MD 21010

Commander
US Army Ballistic Research Laboratory/
ARRADCOM
ATTN: DRDAR-TSB-S (STINFO)
Aberdeen Proving Ground, MD 21005

Commander
US Army Electronics Research
& Development Command
ATTN: DRDEL-CCM (W. H. Pepper)
Adelphi, MD 20783

Commander
US Army Electronics Research
& Development Command
ATTN: DRDEL-CG/DRDEL-DC/DRDEL-CS
2800 Powder Mill Road
Adelphi, MD 20783

Commander
US Army Electronics Research
& Development Command
ATTN: DRDEL-CT
2800 Powder Mill Road
Adelphi, MD 20783

Commander
US Army Electronics Research
& Development Command
ATTN: DRDEL-PAO (M. Singleton)
2800 Powder Mill Road
Adelphi, MD 20783

Project Manager
Smoke/Obscurants
ATTN: DRDPM-SMK
(Dr. Anthony Van de Wal, Jr.)
Aberdeen Proving Ground, MD 21005

Project Manager
Smoke/Obscurants
ATTN: DRDPM-SMK-T (Mr. Sidney Gerard)
Aberdeen Proving Ground, MD 21005

Commander
US Army Test & Evaluation Command
ATTN: DRSTE-AD-M (Mr. Warren M. Baity)
Aberdeen Proving Ground, MD 21005

Commander
US Army Test & Evaluation Command
ATTN: DRSTE-AD-M (Dr. Norman E. Pentz)
Aberdeen Proving Ground, MD 21005

Director
US Army Materiel Systems Analysis Activity
ATTN: DRXSY-AAM (Mr. William Smith)
Aberdeen Proving Ground, MD 21005

Director
US Army Materiel Systems Analysis Activity
ATTN: DRXSY-CS (Mr. Philip H. Beavers)
Aberdeen Proving Ground, MD 21005

Director
US Army Materiel Systems Analysis Activity
ATTN: DRXSY-GB (Wilbur L. Warfield)
Aberdeen Proving Ground, MD 21005

Director
US Army Materiel Systems Analysis Activity
ATTN: DRXSY-GP (Mr. Fred Campbell)
Aberdeen Proving Ground, MD 21005

Director
US Army Material Systems Analysis Activity
ATTN: DRXSY-GP (H. Stamper)
Aberdeen Proving Grounds, MD 21005

Director
US Army Materiel Systems Analysis Activity
ATTN: DRXSY-GS
(Mr. Michael Starks/Mr. Julian Chernick)
Aberdeen Proving Ground, MD 21005

Director
US Army Materiel Systems Analysis Activity
ATTN: DRXSY-J (Mr James F. O'Bryon)
Aberdeen Proving Ground, MD 21005

Director
US Army Materiel Systems Analysis Activity
ATTN: DRXSY-LM (Mr. Robert M. Marchetti)
Aberdeen Proving Ground, MD 21005

Commander
Harry Diamond Laboratories
ATTN: Dr. William W. Carter
2800 Powder Mill Road
Adelphi, MD 20783

Commander
Harry Diamond Laboratories
ATTN: DELHD-R-CM (Mr. Robert McCoskey)
2800 Powder Mill Road
Adelphi, MD 20783

Commander
Harry Diamond Laboratories
ATTN: DELHD-R-CM-NM (Dr. Robert Humphrey)
2800 Powder Mill Road
Adelphi, MD 20783

Commander
Harry Diamond Laboratories
ATTN: DELHD-R-CM-NM (Dr. Z. G. Sztankay)
2800 Powder Mill Road
Adelphi, MD 20783

Commander
Harry Diamond Laboratories
ATTN: DELHD-R-CM-NM (Dr. Joseph Nemarich)
2800 Powder Mill Road
Adelphi, MD 20783

Commander
Air Force Systems Command
ATTN: WER (Mr. Richard F. Picanso)
Andrews AFB, MD 20334

Martin Marietta Laboratories
ATTN: Jar Mo Chen
1450 South Rolling Road
Baltimore, MD 21227

Commander
US Army Concepts Analysis Agency
ATTN: CSCA-SMC (Mr. Hal E. Hock)
8120 Woodmont Avenue
Bethesda, MD 20014

Director
National Security Agency
ATTN: R52/Dr. Douglas Woods
Fort George G. Meade, MD 20755

Chief
Intelligence Materiel Development
& Support Office
US Army Electronic Warfare Laboratory
ATTN: DELEW-I (LTC Kenneth E. Thomas)
Fort George G. Meade, MD 20755

The Johns Hopkins University
Applied Physics Laboratory
ATTN: Dr. Michael J. Lun
John Hopkins Road
Laurell, MD 20810

Dr. Stephen T. Hanley
1720 Rhodesia Avenue
Oxon Hill, MD 20022

Science Applications Inc.
ATTN: Mr. G. D. Currie
15 Research Drive
Ann Arbor, MI 48103

Science Applications Inc.
ATTN: Dr. Robert E. Turner
15 Research Drive
Ann Arbor, MI 48103

Commander
US Army Tank-Automotive Research
& Development Command
ATTN: DRDTA-ZSC (Mr. Harry Young)
Warren, MI 48090

Commander
US Army Tank Automotive Research
& Development Command
ATTN: DRDTA-ZSC (Mr. Wallace Mick, Jr.)
Warren, MI 48090

Dr. A. D. Belmont
Research Division
Control Data Corporation
P.O. Box 1249
Minneapolis, MN 55440

Director
US Army Engr Waterways Experiment Station
ATTN: WESEN (Mr. James Mason)
P.O. Box 631
Vicksburg, MS 39180

Dr. Jerry Davis
Department of Marine, Earth
and Atmospheric Sciences
North Carolina State University
Raleigh, NC 27650

Commander
US Army Research Office
ATTN: DRXRO-GS (Dr. Leo Alpert)
P.O. Box 12211
Research Triangle Park, NC 27709

Commander
US Army Research Office
ATTN: DRXRO-PP (Brenda Mann)
P.O. Box 12211
Research Triangle Park, NC 27709

Commander
US Army Cold Regions Research
& Engineering Laboratory
ATTN: CRREL-RD (Dr. K. F. Sterrett)
Hanover, NH 03755

Commander/Director
US Army Cold Regions Research
& Engineering Laboratory
ATTN: CRREL-RG (Mr. George Aitken)
Hanover, NH 03755

Commander
US Army Cold Regions Research
& Engineering Laboratory
ATTN: CRREL-RG (Mr. Roger H. Berger)
Hanover, NH 03755

Commander
US Army Armament Research
& Development Command
ATTN: DRDAR-AC (Mr. James Greenfield)
Dover, NJ 07801

Commander
US Army Armament Research
& Development Command
ATTN: DRDAR-TSS (Bldg #59)
Dover, NJ 07801

Commander
US Army Armament Research
& Development Command
ATTN: DRCPM-CAWS-EI (Mr. Peteris Jansons)
Dover, NJ 07801

Commander
US Army Armament Research
& Development Command
ATTN: DRCPM-CAWS-EI (Mr. G. H. Waldron)
Dover, NJ 07801

Deputy Joint Project Manager
for Navy/USMC SAL GP
ATTN: DRCPM-CAWS-NV (CPT Joseph Miceli)
Dover, NJ 07801

Commander/Director
US Army Combat Surveillance & Target
Acquisition Laboratory
ATTN: DELCS-I (Mr. David Longinotti)
Fort Monmouth, NJ 07703

Commander/Director
US Army Combat Surveillance & Target
Acquisition Laboratory
ATTN: DELCS-PE (Mr. Ben A. Di Campli)
Fort Monmouth, NJ 07703

Commander/Director
US Army Combat Surveillance & Target
Acquisition Laboratory
ATTN: DELCS-R-S (Mr. Donald L. Foiani)
Fort Monmouth, NJ 07703

Director
US Army Electronics Technology &
Devices Laboratory
ATTN: DELET-DD (S. Danko)
Fort Monmouth, NJ 07703

Project Manager
FIREFINDER/REMBASS
ATTN: DRCPM-FFR-TM (Mr. John M. Bialo)
Fort Monmouth, NJ 07703

Commander
US Army Electronics Research
& Development Command
ATTN: DRDEL-SA (Dr. Walter S. McAfee)
Fort Monmouth, NJ 07703

OLA, 2WS (MAC)
Holloman AFB, NM 88330
Commander
Air Force Weapons Laboratory
ATTN: AFWL/WE (MAJ John R. Elrick)
Kirtland, AFB, NM 87117

Director
USA TRADOC Systems Analysis Activity
ATTN: ATAA-SL
White Sands Missile Range, NM 88002

Director
USA TRADOC Systems Analysis Activity
ATTN: ATAA-SL (Dolores Anguiano)
White Sands Missile Range, NM 88002

Director
USA TRADOC Systems Analysis Activity
ATTN: ATAA-TDB (Mr. Louie Dominguez)
White Sands Missile Range, NM 88002

Director
USA TRADOC Systems Analysis Activity
ATTN: ATAA-TDB (Mr. William J. Leach)
White Sands Missile Range, NM 88002

Director
USA TRADOC Systems Analysis Activity
ATTN: ATAA-TGP (Mr. Roger F. Willis)
White Sands Missile Range, NM 88002

Director
Office of Missile Electronic Warfare
ATTN: DELEW-M-STO (Dr. Steven Kovel)
White Sands Missile Range, NM 88002

Office of the Test Director
Joint Services EO GW CM Test Program
ATTN: DPXDE-TD (Mr. Weldon Findley)
White Sands Missile Range, NM 88002

Commander
US Army White Sands Missile Range
ATTN: STEWS-PT-AL (Laurel B. Saunders)
White Sands Missile Range, NM 88002

Commander
US Army R&D Coordinator
US Embassy - Bonn
Box 165
APO New York 09080

Grumman Aerospace Corporation
Research Department - MS A08-35
ATTN: John E. A. Selby
Bethpage, NY 11714

Rome Air Development Center
ATTN: Documents Library
TSLD (Bette Smith)
Griffiss AFB, NY 13441

Dr. Roberto Vaglio-Laurin
Faculty of Arts and Science
Dept. of Applied Science
26-36 Stuyvesant Street
New York, NY 10003

Air Force Wright Aeronautical Laboratories/
Avionics Laboratory
ATTN: AFWAL/AARI-3 (Mr. Harold Geltmacher)
Wright-Patterson AFB, OH 45433

Air Force Wright Aeronautical Laboratories/
Avionics Laboratory
ATTN: AFWAL/AARI-3 (CPT William C. Smith)
Wright-Patterson AFB, OH 45433

Commandant
US Army Field Artillery School
ATTN: ATSF-CF-R (CPT James M. Watson)
Fort Sill, OK 73503

Commandant
US Army Field Artillery School
ATTN: ATSF-CD-MS
Fort Sill, OK 73503

Commandant
US Army Field Artillery School
ATTN: ATSF-CF-R
Fort Sill, OK 73503

Commandant
US Army Field Artillery School
ATTN: NOAA Liaison Officer
(CDR Jeffrey G. Carlen)
Fort Sill, OK 73503

Commandant
US Army Field Artillery School
Morris Swett Library
ATTN: Reference Librarian
Fort Sill, OK 73503

Commander
Naval Air Development Center
ATTN: Code 301 (Mr. George F. Eck)
Warminster, PA 18974

The University of Texas at El Paso
Electrical Engineering Department
ATTN: Dr. Joseph H. Pierluissi
El Paso, TX 79968

Commandant
US Army Air Defense School
ATTN: ATSA-CD-SC-A (CPT Charles T. Thorn)
Fort Bliss, TX 79916

Commander
HQ, TRADOC Combined Arms Test Activity
ATTN: ATCAT-OP-Q (CPT Henry C. Cobb, Jr.)
Fort Hood, TX 76544

Commander
HQ, TRADOC Combined Arms Test Activity
ATTN: ATCAT-SCI (Dr. Darrell W. Collier)
Fort Hood, TX 76544

Commander
US Army Dugway Proving Ground
ATTN: STEDP-MT-DA-L
Dugway, UT 84022

Commander
US Army Dugway Proving Ground
ATTN: STEDP-MT-DA-M (Mr. Paul E. Carlson)
Dugway, UT 84022

Commander
US Army Dugway Proving Ground
ATTN: STEDP-MT-DA-T (Mr. John Trethewey)
Dugway, UT 84022

Commander
US Army Dugway Proving Ground
ATTN: STEDP-MT-DA-T (Mr. William Peterson)
Dugway, UT 84022

Defense Documentation Center
ATTN: DDC-TCA
Cameron Station Bldg 5
Alexandria, VA 22314
12

Ballistic Missile Defense Program Office
ATTN: DACS-BMT (Colonel Harry F. Ennis)
5001 Eisenhower Avenue
Alexandria, VA 22333

Defense Technical Information Center
ATTN: DDA-2 (Mr. James E. Shafer)
Cameron Station, Bldg 5
Alexandria, VA 22314

Commander
US Army Materiel Development
& Readiness Command
ATTN: DRCBSI-SE (Mr. Albert Giambalvo)
5001 Eisenhower Avenue
Alexandria, VA 22333

Commander
US Army Materiel Development
& Readiness Command
ATTN: DRCLDC (Mr. James Bender)
5001 Eisenhower Avenue
Alexandria, VA 22333

Defense Advanced Rsch Projects Agency
ATTN: Steve Zakanyez
1400 Wilson Blvd
Arlington, VA 22209

Defense Advanced Rsch Projects Agency
ATTN: Dr. James Tegnelia
1400 Wilson Blvd
Arlington, VA 22209

Institute for Defense Analyses
ATTN: Mr. Lucien M. Biberman
400 Army-Navy Drive
Arlington, VA 22202

Institute for Defense Analyses
ATTN: Dr. Ernest Bauer
400 Army-Navy Drive
Arlington, VA 22202

Institute for Defense Analyses
ATTN: Dr. Hans G. Wolfhard
400 Army-Navy Drive
Arlington, VA 22202

System Planning Corporation
ATTN: Mr. Daniel Friedman
1500 Wilson Boulevard
Arlington, VA 22209

System Planning Corporation
ATTN: COL Hank Shelton
1500 Wilson Boulevard
Arlington, VA 22209

US Army Intelligence & Security Command
ATTN: Edwin Speakman, Scientific Advisor
Arlington Hall Station
Arlington, VA 22212

Commander
US Army Operational Test
& Evaluation Agency
ATTN: CSTE-ED (Mr. Floyd I. Hill)
5600 Columbia Pike
Falls Church, VA 22041

Commander and Director
US Army Engineer Topographic Laboratories
ATTN: ETL-GS-A (Mr. Thomas Neidringhaus)
Fort Belvoir, VA 22060

Director
US Army Night Vision &
Electro-Optics Laboratory
ATTN: DELNV-L (Dr. Rudolf G. Buser)
Fort Belvoir, VA 22060

Director
US Army Night Vision &
Electro-Optics Laboratory
ATTN: DELNV-L (Dr. Robert S. Rodhe)
Fort Belvoir, VA 22060

Director
US Army Night Vision &
Electro-Optics Laboratory
ATTN: DELNV-VI (Mr. Joseph R. Moulton)
Fort Belvoir, VA 22060

Director
US Army Night Vision &
Electro-Optics Laboratory
ATTN: DELNV-VI (Luanne P. Obert)
Fort Belvoir, VA 22060

Director
US Army Night Vision
& Electro-Optics Laboratory
ATTN: DELNV-VI (Mr. Thomas W. Cassidy)
Fort Belvoir, VA 22060

Director
US Army Night Vision &
Electro-Optics Laboratory
ATTN: DELNV-VI (Mr. Richard J. Bergemann)
Fort Belvoir, VA 22060

Director
US Army Night Vision &
Electro-Optics Laboratory
ATTN: DELNV-VI (Dr. James A. Ratches)
Fort Belvoir, VA 22060

Commander
US Army Training & Doctrine Command
ATTN: ATCD-AN
Fort Monroe, VA 23651

Commander
US Army Training & Doctrine Command
ATTN: ATCD-AN-M
Fort Monroe, VA 23651

Commander
US Army Training & Doctrine Command
ATTN: ATCD-F-A (Mr. Chris O'Connor, Jr.)
Fort Monroe, VA 23651

Commander
US Army Training & Doctrine Command
ATTN: ATCD-IE-R (Mr. David M. Ingram)
Fort Monroe, VA 23651

Commander
US Army Training & Doctrine Command
ATTN: ATCD-M-I/ATCD-M-A
Fort Monroe, VA 23651

Commander
US Army Training & Doctrine Command
ATTN: ATDOC-TA (Dr. Marvin P. Pastel)
Fort Monroe, VA 23651

Department of the Air Force
OL-I, AWS
Fort Monroe, VA 23651

Department of the Air Force
HQS 5 Weather Wing (MAC)
ATTN: 5 WW/DN
Langley Air Force Base, VA 23655

Commander
US Army INSCOM/Quest Research Corporation
ATTN: Mr. Donald Wilmot
6845 Elm Street, Suite 407
McLean, VA 22101

General Research Corporation
ATTN: Dr. Ralph Zirkind
7655 Old Springhouse Road
McLean, VA 22102

Science Applications, Inc.
8400 Westpark Drive
ATTN: Dr. John E. Cockayne
McLean, VA 22102

US Army Nuclear & Chemical Agency
ATTN: MONA-WE (Dr. John A. Berberet)
7500 Backlick Road, Bldg 2073
Springfield, VA 22150

Director
US Army Signals Warfare Laboratory
ATTN: DELSW-EA (Mr. Douglas Harkleroad)
Vint Hill Farms Station
Warrenton, VA 22186

Director
US Army Signals Warfare Laboratory
ATTN: DELSW-OS (Dr. Royal H. Burkhardt)
Vint Hill Farms Station
Warrenton, VA 22186

Commander
US Army Cold Regions Test Center
ATTN: STECR-TD (Mr. Jerold Barger)
APO Seattle, WA 98733

HQDA (SAUS-OR/Hunter M. Woodall, Jr./
Dr. Herbert K. Fallin)
Rm 2E 614, Pentagon
Washington, DC 20301

COL Elbert W. Friday, Jr.
OUSDRE
Rm 3D 129, Pentagon
Washington, DC 20301

Defense Communications Agency
Technical Library Center
Code 222
Washington, DC 20305

Director
Defense Nuclear Agency
ATTN: Technical Library (Mrs. Betty Fox)
Washington, DC 20305

Director
Defense Nuclear Agency
ATTN: RAAE (Dr. Carl Fitz)
Washington, DC 20305

Director
Defense Nuclear Agency
ATTN: SPAS (Mr. Donald J. Kohler)
Washington, DC 20305

Defense Intelligence Agency
ATTN: DT/AC (LTC Robert Poplawski)
Washington, DC 20301

HQDA (DAMA-ARZ-D/Dr. Verderame)
Washington, DC 20310

HQDA (DAMI-ISP/Mr. Beck)
Washington, DC 20310

Department of the Army
Deputy Chief of Staff for
Operations and Plans
ATTN: DAMO-RQ
Washington, DC 20310

Department of the Army
Director of Telecommunications and
Command and Control
ATTN: DAMO-TCZ
Washington, DC 20310

Department of the Army
Assistant Chief of Staff for Intelligence
ATTN: DAMI-TS
Washington, DC 20310

HQDA (DAEN-RDM/Dr. de Percin)
Casimir Pulaski Building
20 Massachusetts Avenue
Room 6203
Washington, DC 20314

National Science Foundation
Division of Atmospheric Sciences
ATTN: Dr. Eugene W. Bierly
1800 G. Street, N.W.
Washington, DC 20550

Director
Naval Research Laboratory
ATTN: Code 4320 (Dr. Lothar H. Ruhnke)
Washington, DC 20375

Commanding Officer
Naval Research Laboratory
ATTN: Code 6009 (Dr. John MacCallum, Jr.)
Washington, DC 20375

Commanding Officer
Naval Research Laboratory
ATTN: Code 6530 (Mr. Raymond A. Patten)
Washington, DC 20375

Commanding Officer
Naval Research Laboratory
ATTN: Code 6533 (Dr. James A. Dowling)
Washington, DC 20375

ATMOSPHERIC SCIENCES RESEARCH REPORTS

1. Lindberg, J. D. "An Improvement to a Method for Measuring the Absorption Coefficient of Atmospheric Dust and other Strongly Absorbing Powders," ECOM-5565, July 1975.

2. Avara, Elton P., "Mesoscale Wind Shears Derived from Thermal Winds," ECOM-5566, July 1975.

3. Gomez, Richard B., and Joseph H. Pierluissi, "Incomplete Gamma Function Approximation for King's Strong-Line Transmittance Model," ECOM-5567, July 1975.

4. Blanco, A. J., and B. F. Engebos, "Ballistic Wind Weighting Functions for Tank Projectiles," ECOM-5568, August 1975.

5. Taylor, Fredrick J., Jack Smith, and Thomas H. Pries, "Crosswind Measurements through Pattern Recognition Techniques," ECOM-5569, July 1975.

6. Walters, D. L., "Crosswind Weighting Functions for Direct-Fire Projectiles," ECOM-5570, August 1975.

7. Duncan, Louis D., "An Improved Algorithm for the Iterated Minimal Information Solution for Remote Sounding of Temperature," ECOM-5571, August 1975.

8. Robbiani, Raymond L., "Tactical Field Demonstration of Mobile Weather Radar Set AN/TPS-41 at Fort Rucker, Alabama," ECOM-5572, August 1975.

9. Miers, B., G. Blackman, D. Langer, and N. Lorimier, "Analysis of SMS/GOES Film Data," ECOM-5573, September 1975.

10. Manquero, Carlos, Louis Duncan, and Rufus Bruce, "An Indication from Satellite Measurements of Atmospheric CO_2 Variability," ECOM-5574, September 1975.

11. Petracca, Carmine, and James D. Lindberg, "Installation and Operation of an Atmospheric Particulate Collector," ECOM-5575, September 1975.

12. Avara, Elton P., and George Alexander, "Empirical Investigation of Three Iterative Methods for Inverting the Radiative Transfer Equation," ECOM-5576, October 1975.

13. Alexander, George D., "A Digital Data Acquisition Interface for the SMS Direct Readout Ground Station - Concept and Preliminary Design," ECOM-5577, October 1975.

14. Cantor, Israel, "Enhancement of Point Source Thermal Radiation Under Clouds in a Nonattenuating Medium," ECOM-5578, October 1975.

15. Norton, Colburn, and Glenn Hoidale, "The Diurnal Variation of Mixing Height by Month over White Sands Missile Range, NM," ECOM-5579, November 1975.

16. Avara, Elton P., "On the Spectrum Analysis of Binary Data," ECOM-5580, November 1975.

17. Taylor, Fredrick J., Thomas H. Pries, and Chao-Huan Huang, "Optimal Wind Velocity Estimation," ECOM-5581, December 1975.

18. Avara, Elton P., "Some Effects of Autocorrelated and Cross-Correlated Noise on the Analysis of Variance," ECOM-5582, December 1975.

19. Gillespie, Patti S., R. L. Armstrong, and Kenneth O. White, "The Spectral Characteristics and Atmospheric CO_2 Absorption of the Ho^{+3}:YLF Laser at 2.05μm," ECOM-5583, December 1975.

20. Novlan, David J., "An Empirical Method of Forecasting Thunderstorms for the White Sands Missile Range," ECOM-5584, February 1976.

21. Avara, Elton P., "Randomization Effects in Hypothesis Testing with Autocorrelated Noise," ECOM-5585, February 1976.

22. Watkins, Wendell R., "Improvements in Long Path Absorption Cell Measurement," ECOM-5586, March 1976.

23. Thomas, Joe, George D. Alexander, and Marvin Dubbin, "SATTEL - An Army Dedicated Meteorological Telemetry System," ECOM-5587, March 1976.

24. Kennedy, Bruce W., and Delbert Bynum, "Army User Test Program for the RDT&E-XM-75 Meteorological Rocket," ECOM-5588, April 1976.

25. Barnett, Kenneth M., "A Description of the Artillery Meteorological Comparisons at White Sands Missile Range, October 1974 - December 1974 ('PASS' - Prototype Artillery [Meteorological] Subsystem)," ECOM-5589, April 1976.

26. Miller, Walter B., "Preliminary Analysis of Fall-of-Shot from Project 'PASS'," ECOM-5590, April 1976.

27. Avara, Elton P., "Error Analysis of Minimum Information and Smith's Direct Methods for Inverting the Radiative Transfer Equation," ECOM-5591, April 1976.

28. Yee, Young P., James D. Horn, and George Alexander, "Synoptic Thermal Wind Calculations from Radiosonde Observations Over the Southwestern United States," ECOM-5592, May 1976.

29. Duncan, Louis D., and Mary Ann Seagraves, "Applications of Empirical Corrections to NOAA-4 VTPR Observations," ECOM-5593, May 1976.

30. Miers, Bruce T., and Steve Weaver, "Applications of Meteorological Satellite Data to Weather Sensitive Army Operations," ECOM-5594, May 1976.

31. Sharenow, Moses, "Redesign and Improvement of Balloon ML-566," ECOM-5595, June 1976.

32. Hansen, Frank V., "The Depth of the Surface Boundary Layer," ECOM-5596, June 1976.

33. Pinnick, R. G., and E. B. Stenmark, "Response Calculations for a Commerical Light-Scattering Aerosol Counter," ECOM-5597, July 1976.

34. Mason, J., and G. B. Hoidale, "Visibility as an Estimator of Infrared Transmittance," ECOM-5598, July 1976.

35. Bruce, Rufus E., Louis D. Duncan, and Joseph H. Pierluissi, "Experimental Study of the Relationship Between Radiosonde Temperatures and Radiometric-Area Temperatures," ECOM-5599, August 1976.

36. Duncan, Louis D., "Stratospheric Wind Shear Computed from Satellite Thermal Sounder Measurements," ECOM-5800, September 1976.

37. Taylor, F., P. Mohan, P. Joseph, and T. Pries, "An All Digital Automated Wind Measurement System," ECOM-5801, September 1976.

38. Bruce, Charles, "Development of Spectrophones for CW and Pulsed Radiation Sources," ECOM-5802, September 1976.

39. Duncan, Louis D., and Mary Ann Seagraves, "Another Method for Estimating Clear Column Radiances," ECOM-5803, October 1976.

40. Blanco, Abel J., and Larry E. Taylor, "Artillery Meteorological Analysis of Project Pass," ECOM-5804, October 1976.

41. Miller, Walter, and Bernard Engebos, "A Mathematical Structure for Refinement of Sound Ranging Estimates," ECOM-5805, November 1976.

42. Gillespie, James B., and James D. Lindberg, "A Method to Obtain Diffuse Reflectance Measurements from 1.0 and 3.0μm Using a Cary 17I Spectrophotometer," ECOM-5806, November 1976.

43. Rubio, Roberto, and Robert O. Olsen, "A Study of the Effects of Temperature Variations on Radio Wave Absorption," ECOM-5807, November 1976.

44. Ballard, Harold N., "Temperature Measurements in the Stratosphere from Balloon-Borne Instrument Platforms, 1968-1975," ECOM-5808, December 1976.

45. Monahan, H. H., "An Approach to the Short-Range Prediction of Early Morning Radiation Fog," ECOM-5809, January 1977.

46. Engebos, Bernard Francis, "Introduction to Multiple State Multiple Action Decision Theory and Its Relation to Mixing Structures," ECOM-5810, January 1977.

47. Low, Richard D. H., "Effects of Cloud Particles on Remote Sensing from Space in the 10-Micrometer Infrared Region," ECOM-5811, January 1977.

48. Bonner, Robert S., and R. Newton, "Application of the AN/GVS-5 Laser Rangefinder to Cloud Base Height Measurements," ECOM-5812, February 1977.

49. Rubio, Roberto, "Lidar Detection of Subvisible Reentry Vehicle Erosive Atmospheric Material," ECOM-5813, March 1977.

50. Low, Richard D. H., and J. D. Horn, "Mesoscale Determination of Cloud-Top Height: Problems and Solutions," ECOM-5814, March 1977.

51. Duncan, Louis D., and Mary Ann Seagraves, "Evaluation of the NOAA-4 VTPR Thermal Winds for Nuclear Fallout Predictions," ECOM-5815, March 1977.

52. Randhawa, Jagir S., M. Izquierdo, Carlos McDonald, and Zvi Salpeter, "Stratospheric Ozone Density as Measured by a Chemiluminescent Sensor During the Stratcom VI-A Flight," ECOM-5816, April 1977.

53. Rubio, Roberto, and Mike Izquierdo, "Measurements of Net Atmospheric Irradiance in the 0.7- to 2.8-Micrometer Infrared Region," ECOM-5817, May 1977.

54. Ballard, Harold N., Jose M. Serna, and Frank P. Hudson, Consultant for Chemical Kinetics, "Calculation of Selected Atmospheric Composition Parameters for the Mid-Latitude, September Stratosphere," ECOM-5818, May 1977.

55. Mitchell, J. D., R. S. Sagar, and R. O. Olsen, "Positive Ions in the Middle Atmosphere During Sunrise Conditions," ECOM-5819, May 1977.

56. White, Kenneth O., Wendell R. Watkins, Stuart A. Schleusener, and Ronald L. Johnson, "Solid-State Laser Wavelength Identification Using a Reference Absorber," ECOM-5820, June 1977.

57. Watkins, Wendell R., and Richard G. Dixon, "Automation of Long-Path Absorption Cell Measurements," ECOM-5821, June 1977.

58. Taylor, S. E., J. M. Davis, and J. B. Mason, "Analysis of Observed Soil Skin Moisture Effects on Reflectance," ECOM-5822, June 1977.

59. Duncan, Louis D., and Mary Ann Seagraves, "Fallout Predictions Computed from Satellite Derived Winds," ECOM-5823, June 1977.

60. Snider, D. E., D. G. Murcray, F. H. Murcray, and W. J. Williams, "Investigation of High-Altitude Enhanced Infrared Backround Emissions," (U), SECRET, ECOM-5824, June 1977.

61. Dubbin, Marvin H., and Dennis Hall, "Synchronous Meteorological Satellite Direct Readout Ground System Digital Video Electronics," ECOM-5825, June 1977.

62. Miller, W., and B. Engebos, "A Preliminary Analysis of Two Sound Ranging Algorithms," ECOM-5826, July 1977.

63. Kennedy, Bruce W., and James K. Luers, "Ballistic Sphere Techniques for Measuring Atmospheric Parameters," ECOM-5827, July 1977.

64. Duncan, Louis D., "Zenith Angle Variation of Satellite Thermal Sounder Measurements," ECOM-5828, August 1977.

65. Hansen, Frank V., "The Critical Richardson Number," ECOM-5829, September 1977.

66. Ballard, Harold N., and Frank P. Hudson (Compilers), "Stratospheric Composition Balloon-Borne Experiment," ECOM-5830, October 1977.

67. Barr, William C., and Arnold C. Peterson, "Wind Measuring Accuracy Test of Meteorological Systems," ECOM-5831, November 1977.

68. Ethridge, G. A., and F. V. Hansen, "Atmospheric Diffusion: Similarity Theory and Empirical Derivations for Use in Boundary Layer Diffusion Problems," ECOM-5832, November 1977.

69. Low, Richard D. H., "The Internal Cloud Radiation Field and a Technique for Determining Cloud Blackness," ECOM-5833, December 1977.

70. Watkins, Wendell R., Kenneth O. White, Charles W. Bruce, Donald L. Walters, and James D. Lindberg, "Measurements Required for Prediction of High Energy Laser Transmission," ECOM-5834, December 1977.

71. Rubio, Robert, "Investigation of Abrupt Decreases in Atmospherically Backscattered Laser Energy," ECOM-5835, December 1977.

72. Monahan, H. H., and R. M. Cionco, "An Interpretative Review of Existing Capabilities for Measuring and Forecasting Selected Weather Variables (Emphasizing Remote Means)," ASL-TR-0001, January 1978.

73. Heaps, Melvin G., "The 1979 Solar Eclipse and Validation of D-Region Models," ASL-TR-0002, March 1978.

74. Jennings, S. G., and J. B. Gillespie, "M.I.E. Theory Sensitivity Studies - The Effects of Aerosol Complex Refractive Index and Size Distribution Variations on Extinction and Absorption Coefficients, Part II: Analysis of the Computational Results," ASL-TR-0003, March 1978.

75. White, Kenneth O., et al, "Water Vapor Continuum Absorption in the 3.5μm to 4.0μm Region," ASL-TR-0004, March 1978.

76. Olsen, Robert O., and Bruce W. Kennedy, "ABRES Pretest Atmospheric Measurements," ASL-TR-0005, April 1978.

77. Ballard, Harold N., Jose M. Serna, and Frank P. Hudson, "Calculation of Atmospheric Composition in the High Latitude September Stratosphere," ASL-TR-0006, May 1978.

78. Watkins, Wendell R., et al, "Water Vapor Absorption Coefficients at HF Laser Wavelengths," ASL-TR-0007, May 1978.

79. Hansen, Frank V., "The Growth and Prediction of Nocturnal Inversions," ASL-TR-0008, May 1978.

80. Samuel, Christine, Charles Bruce, and Ralph Brewer, "Spectrophone Analysis of Gas Samples Obtained at Field Site," ASL-TR-0009, June 1978.

81. Pinnick, R. G., et al., "Vertical Structure in Atmospheric Fog and Haze and its Effects on IR Extinction," ASL-TR-0010, July 1978.

82. Low, Richard D. H., Louis D. Duncan, and Richard B. Gomez, "The Microphysical Basis of Fog Optical Characterization," ASL-TR-0011, August 1978.

83. Heaps, Melvin G., "The Effect of a Solar Proton Event on the Minor Neutral Constituents of the Summer Polar Mesosphere," ASL-TR-0012, August 1978.

84. Mason, James B., "Light Attenuation in Falling Snow," ASL-TR-0013, August 1978.

85. Blanco, Abel J., "Long-Range Artillery Sound Ranging: 'PASS' Meteorological Application," ASL-TR-0014, September 1978.

86. Heaps, M. G., and F. E. Niles, "Modeling of Ion Chemistry of the D-Region: A Case Study Based Upon the 1966 Total Solar Eclipse," ASL-TR-0015, September 1978.

87. Jennings, S. G., and R. G. Pinnick, "Effects of Particulate Complex Refractive Index and Particle Size Distribution Variations on Atmospheric Extinction and Absorption for Visible Through Middle-Infrared Wavelengths," ASL-TR-0016, September 1978.

88. Watkins, Wendell R., Kenneth O. White, Lanny R. Bower, and Brian Z. Sojka, "Pressure Dependence of the Water Vapor Continuum Absorption in the 3.5- to 4.0-Micrometer Region," ASL-TR-0017, September 1978.

89. Miller, W. B., and B. F. Engebos, "Behavior of Four Sound Ranging Techniques in an Idealized Physical Environment," ASL-TR-0018, September 1978.

90. Gomez, Richard G., "Effectiveness Studies of the CBU-88/B Bomb, Cluster, Smoke Weapon," (U), CONFIDENTIAL ASL-TR-0019, September 1978.

91. Miller, August, Richard C. Shirkey, and Mary Ann Seagraves, "Calculation of Thermal Emission from Aerosols Using the Doubling Technique," ASL-TR-0020, November 1978.

92. Lindberg, James D., et al, "Measured Effects of Battlefield Dust and Smoke on Visible, Infrared, and Millimeter Wavelengths Propagation: A Preliminary Report on Dusty Infrared Test-I (DIRT-I)," ASL-TR-0021, January 1979.

93. Kennedy, Bruce W., Arthur Kinghorn, and B. R. Hixon, "Engineering Flight Tests of Range Meteorological Sounding System Radiosonde," ASL-TR-0022, February 1979.

94. Rubio, Roberto, and Don Hoock, "Microwave Effective Earth Radius Factor Variability at Wiesbaden and Balboa," ASL-TR-0023, February 1979.

95. Low, Richard D. H., "A Theoretical Investigation of Cloud/Fog Optical Properties and Their Spectral Correlations, "ASL-TR-0024, February 1979.

96. Pinnick, R. G., and H. J. Auvermann, "Response Characteristics of Knollenberg Light-Scattering Aerosol Counters," ASL-TR-0025, February 1979.

97. Heaps, Melvin G., Robert O. Olsen, and Warren W. Berning, "Solar Eclipse 1979, Atmospheric Sciences Laboratory Program Overview," ASL-TR-0026, February 1979.

98. Blanco, Abel J., "Long-Range Artillery Sound Ranging: 'PASS' GR-8 Sound Ranging Data," ASL-TR-0027, March 1979.

99. Kennedy, Bruce W., and Jose M. Serna, "Meteorological Rocket Network System Reliability," ASL-TR-0028, March 1979.

100. Swingle, Donald M., "Effects of Arrival Time Errors in Weighted Range Equation Solutions for Linear Base Sound Ranging," ASL-TR-0029, April 1979.

101. Umstead, Robert K., Ricardo Pena, and Frank V. Hansen, "KWIK: An Algorithm for Calculating Munition Expenditures for Smoke Screening/Obscuration in Tactical Situations," ASL-TR-0030, April 1979.

102. D'Arcy, Edward M., "Accuracy Validation of the Modified Nike Hercules Radar," ASL-TR-0031, May 1979.

103. Rodriguez, Ruben, "Evaluation of the Passive Remote Crosswind Sensor," ASL-TR-0032, May 1979.

104. Barber, T. L., and R. Rodriguez, "Transit Time Lidar Measurement of Near-Surface Winds in the Atmosphere," ASL-TR-0033, May 1979.

105. Low, Richard D. H., Louis D. Duncan, and Y. Y. Roger R. Hsiao, "Microphysical and Optical Properties of California Coastal Fogs at Fort Ord," ASL-TR-0034, June 1979.

106. Rodriguez, Ruben, and William J. Vechione, "Evaluation of the Saturation Resistant Crosswind Sensor," ASL-TR-0035, July 1979.

107. Ohmstede, William D., "The Dynamics of Material Layers," ASL-TR-0036, July 1979.

108. Pinnick, R. G., S. G. Jennings, Petr Chylek, and H. J. Auvermann, "Relationships between IR Extinction Absorption, and Liquid Water Content of Fogs," ASL-TR-0037, August 1979.

109. Rodriguez, Ruben, and William J. Vechione, "Performance Evaluation of the Optical Crosswind Profiler," ASL-TR-0038, August 1979.

110. Miers, Bruce T., "Precipitation Estimation Using Satellite Data," ASL-TR-0039, September 1979.

111. Dickson, David H., and Charles M. Sonnenschein, "Helicopter Remote Wind Sensor System Description," ASL-TR-0040, September 1979.

112. Heaps, Melvin G., and Joseph M. Heimerl, "Validation of the Dairchem Code, I: Quiet Midlatitude Conditions," ASL-TR-0041, September 1979.

113. Bonner, Robert S., and William J. Lentz, "The Visioceilometer: A Portable Cloud Height and Visibility Indicator," ASL-TR-0042, October 1979.

114. Cohn, Stephen L., "The Role of Atmospheric Sulfates in Battlefield Obscurations," ASL-TR-0043, October 1979.

115. Fawbush, E. J., et al, "Characterization of Atmospheric Conditions at the High Energy Laser System Test Facility (HELSTF), White Sands Missile Range, New Mexico, Part I, 24 March to 8 April 1977," ASL-TR-0044, November 1979.

116. Barber, Ted L., "Short-Time Mass Variation in Natural Atmospheric Dust," ASL-TR-0045, November 1979.

117. Low, Richard D. H., "Fog Evolution in the Visible and Infrared Spectral Regions and its Meaning in Optical Modeling," ASL-TR-0046, December 1979.

118. Duncan, Louis D., et al, "The Electro-Optical Systems Atmospheric Effects Library, Volume I: Technical Documentation," ASL-TR-0047, December 1979.

119. Shirkey, R. C., et al, "Interim E-O SAEL, Volume II, Users Manual," ASL-TR-0048, December 1979.

120. Kobayashi, H. K., "Atmospheric Effects on Millimeter Radio Waves," ASL-TR-0049, January 1980.

121. Seagraves, Mary Ann, and Louis D. Duncan, "An Analysis of Transmittances Measured Through Battlefield Dust Clouds," ASL-TR-0050, February 1980.

122. Dickson, David H., and Jon E. Ottesen, "Helicopter Remote Wind Sensor Flight Test," ASL-TR-0051, February 1980.

123. Pinnick, R. G., and S. G. Jennings, "Relationships Between Radiative Properties and Mass Content of Phosphoric Acid, HC, Petroleum Oil, and Sulfuric Acid Military Smokes," ASL-TR-0052, April 1980.

124. Hinds, B. D., and J. B. Gillespie, "Optical Characterization of Atmospheric Particulates on San Nicolas Island, California," ASL-TR-0053, April 1980.

125. Miers, Bruce T., "Precipitation Estimation for Military Hydrology," ASL-TR-0054, April 1980.

126. Stenmark, Ernest B., "Objective Quality Control of Artillery Computer Meteorological Messages," ASL-TR-0055, April 1980.

127. Duncan, Louis D., and Richard D. H. Low, "Bimodal Size Distribution Models for Fogs at Meppen, Germany," ASL-TR-0056, April 1980.

128. Olsen, Robert O., and Jagir S. Randhawa, "The Influence of Atmospheric Dynamics on Ozone and Temperature Structure," ASL-TR-0057, May 1980.

129. Kennedy, Bruce W., et al, "Dusty Infrared Test-II (DIRT-II) Program," ASL-TR-0058, May 1980.

130. Heaps, Melvin G., Robert O. Olsen, Warren Berning, John Cross, and Arthur Gilcrease, "1979 Solar Eclipse, Part I - Atmospheric Sciences Laboratory Field Program Summary," ASL-TR-0059, May 1980

131. Miller, Walter B., "User's Guide for Passive Target Acquisition Program Two (PTAP-2)," ASL-TR-0060, June 1980.

132. Holt, E. H., editor, "Atmospheric Data Requirements for Battlefield Obscuration Applications," ASL-TR-0061, June 1980.

133. Shirkey, Richard C., August Miller, George H. Goedecke, and Yugal Behl, "Single Scattering Code AGAUSX: Theory, Applications, Comparisons, and Listing," ASL-TR-0062, July 1980.

134. Sojka, Brian Z., and Kenneth O. White, "Evaluation of Specialized Photoacoustic Absorption Chambers for Near-Millimeter Wave (NMMW) Propagation Measurements," ASL-TR-0063, August 1980.

135. Bruce, Charles W., Young Paul Yee, and S. G. Jennings, "In Situ Measurement of the Ratio of Aerosol Absorption to Extinction Coefficient," ASL-TR-0064, August 1980.

136. Yee, Young Paul, Charles W. Bruce, and Ralph J. Brewer, "Gaseous/Particulate Absorption Studies at WSMR using Laser Sourced Spectrophones," ASL-TR-0065, June 1980.

137. Lindberg, James D., Radon B. Loveland, Melvin Heaps, James B. Gillespie, and Andrew F. Lewis, "Battlefield Dust and Atmospheric Characterization Measurements During West German Summertime Conditions in Support of Grafenwohr Tests," ASL-TR-0066, September 1980.

138. Vechione, W. J., "Evaluation of the Environmental Instruments, Incorporated Series 200 Dual Component Wind Set," ASL-TR-0067, September 1980.

139. Bruce, C. W., Y. P. Yee, B. D. Hinds, R. G. Pinnick, R. J. Brewer, and J. Minjares, "Initial Field Measurements of Atmospheric Absorption at 9μm to 11μm Wavelengths," ASL-TR-0068, October 1980.

140. Heaps, M. G., R. O. Olsen, K. D. Baker, D. A. Burt, L. C. Howlett, L. L. Jensen, E. F. Pound, and G. D. Allred, "1979 Solar Eclipse: Part II Initial Results for Ionization Sources, Electron Density, and Minor Neutral Constituents," ASL-TR-0069, October 1980.

141. Low, Richard D. H., "One-Dimensional Cloud Microphysical Models for Central Europe and their Optical Properties," ASL-TR-0070, October 1980.

142. Duncan, Louis D., James D. Lindberg, and Radon B. Loveland, "An Empirical Model of the Vertical Structure of German Fogs," ASL-TR-0071, November 1980.

143. Duncan, Louis D., "EOSAEL 80, Volume I, Technical Documentation," ASL-TR-0072, January 1981.

144. Shirkey, R. C., and S. G. O'Brien, "EOSAEL 80, Volume II, Users Manual," ASL-TR-0073, January 1981.

145. Bruce, C. W., "Characterization of Aerosol Nonlinear Effects on a High-Power CO_2 Laser Beam," ASL-TR-0074, February 1981.

146. Duncan, Louis D., and James D. Lindberg, "Air Mass Considerations in Fog Optical Modeling," ASL-TR-0075, February 1981.

147. Kunkel, Kenneth E., "Evaluation of a Tethered Kite Anemometer," ASL-TR-0076, February 1981.

148. Kunkel, K. E., et al, "Characterization of Atmospheric Conditions at the High Energy Laser System Test Facility (HELSTF) White Sands Missile Range, New Mexico, August 1977 to October 1978, Part II, Optical Turbulence, Wind, Water Vapor Pressure, Temperature," ASL-TR-0077, February 1981.

149. Miers, Bruce T., "Weather Scenarios for Central Germany," ASL-TR-0078, February 1981.

150. Cogan, James L., "Sensitivity Analysis of a Mesoscale Moisture Model," ASL-TR-0079, March 1981.

151. Brewer, R. J., C. W. Bruce, and J. L. Mater, "Optoacoustic Spectroscopy of C_2H_4 at the 9μm and 10μm $C^{12}O_2^{16}$ Laser Wavelengths," ASL-TR-0080, March 1981.

152. Swingle, Donald M., "Reducible Errors in the Artillery Sound Ranging Solution, Part I: The Curvature Correction" (U), SECRET, ASL-TR-0081, April 1981.

153. Miller, Walter B., "The Existence and Implications of a Fundamental System of Linear Equations in Sound Ranging" (U), SECRET, ASL-TR-0082, April 1981.

154. Bruce, Dorothy, Charles W. Bruce, and Young Paul Yee, "Experimentally Determined Relationship Between Extinction and Liquid Water Content," ASL-TR-0083, April 1981.

155. Seagraves, Mary Ann, "Visible and Infrared Obscuration Effects of Ice Fog," ASL-TR-0084, May 1981.

156. Watkins, Wendell R., and Kenneth O. White, "Wedge Absorption Remote Sensor," ASL-TR-0085, May 1981.

157. Watkins, Wendell R., Kenneth O. White, and Laura J. Crow, "Turbulence Effects on Open Air Multipaths," ASL-TR-0086, May 1981.

158. Blanco, Abel J., "Extending Application of the Artillery Computer Meteorological Message," ASL-TR-0087, May 1981.

159. Heaps, M. G., D. W. Hoock, R. O. Olsen, B. F. Engebos, and R. Rubio, "High Frequency Position Location: An Assessment of Limitations and Potential Improvements," ASL-TR-0088, May 1981.

160. Watkins, Wendell R., and Kenneth O. White, "Laboratory Facility for Measurement of Hot Gaseous Plume Radiative Transfer," ASL-TR-0089, June 1981.

161. Heaps, M. G., "Dust Cloud Models: Sensitivity of Calculated Transmittances to Variations in Input Parameters," ASL-TR-0090, June 1981.

162. Seagraves, Mary Ann, "Some Optical Properties of Blowing Snow," ASL-TR-0091, June 1981.

163. Kobayashi, Herbert K., "Effect of Hail, Snow, and Melting Hydrometeors on Millimeter Radio Waves," ASL-TR-0092, July 1981.

164. Cogan, James L., "Techniques for the Computation of Wind, Ceiling, and Extinction Coefficient Using Currently Acquired RPV Data," ASL-TR-0093, July 1981.

165. Miller, Walter B., and Bernard F. Engebos, "On the Possibility of Improved Estimates for Effective Wind and Temperature," (U), SECRET, ASL-TR-0094, August 1981.

166. Heaps, Melvin G., "The Effect of Ionospheric Variability on the Accuracy of High Frequency Position Location," ASL-TR-0095, August 1981.

167. Sutherland, Robert A., Donald W. Hoock, and Richard B. Gomez, "An Objective Summary of US Army Electro-Optical Modeling and Field Testing in an Obscuring Environment," ASL-TR-0096, October 1981.

168. Pinnick, R. G., et al, "Backscatter and Extinction in Water Clouds," ASL-TR-0097, October 1981.

169. Cole, Henry P., and Melvin G. Heaps, "Properties of Dust as an Electron and Ion Attachment Site for Use in D Region Ion Chemistry," ASL-TR-0098, October 1981.

170. Spellicy, Robert L., Laura J. Crow, and Kenneth O. White, "Water Vapor Absorption Coefficients at HF Laser Wavelengths Part II: Development of the Measurement System and Measurements at Simulated Altitudes to 10 KM," ASL-TR-0099, November 1981.


DATE
FILMED
2-8